Thesis for the Degree of Doctor of Philosophy

Cerebral Hemodynamics through Intracranial Pressure

Sima Shahsavari

To:

Your time is limited, so don't
waste it living someone else's life.

Steve Jobs

Gothenburg, October 2011

Department of Signals and Systems
Signal Processing Group
Chalmers University of Technology
Gothenburg, Sweden 2011

Cerebral Hemodynamics
through Intracranial Pressure

Sima Shahsavari
ISBN 978-91-7385-596-9

Doktorsavhandlingar vid Chalmers Tekniska Högskola
Ny Serie nr 3277
ISSN 0346-718X

Department of Signals and Systems
Signal Processing Group
Chalmers University of Technology
SE-412 96 Gothenburg
Sweden
Phone: +46 (0)31 772 1000

Front cover: Brain Activity Intelligence. Photo by Skypixel. The image was purchased from www.dreamstime.com and edited by the author.

Prepared using LaTeX.
Printed by Chalmers Reproservice
Gothenburg, Sweden, 2011

To my beloved Maziar

Why think thus O men of piety
I have returned to sobriety
I am neither a Moslem nor a Hindu
I am not Christian, Zoroastrian, nor Jew

I am neither of the West nor the East
Not of the ocean, nor an earthly beast
I am neither a natural wonder
Nor from the stars yonder

Neither flesh of dust, nor wind inspire
Nor water in veins, nor made of fire
I am neither an earthly carpet, nor gems terrestrial
Nor am I confined to Creation, nor the Throne Celestial

Not of ancient promises, nor of future prophecy
Not of hellish anguish, nor of paradisic ecstasy
Neither the progeny of Adam, nor Eve
Nor of the world of heavenly make-believe

My place is the no-place
My image is without face
Neither of body nor the soul
I am of the Divine Whole

I eliminated duality with joyous laughter
Saw the unity of here and the hereafter
Unity is what I sing, unity is what I speak
Unity is what I know, unity is what I seek

Molana Jalal-e-Din Mohammad Molavi Rumi
Poem 116 from Divan-e Shams Tabrizi

Cerebral Hemodynamics through Intracranial Pressure

Sima Shahsavari
Department of Signals and Systems
Chalmers University of Technology

Abstract

Traumatic Brain Injury (TBI) continues to be a major problem worldwide. Today, intensive care of patients with TBI is mainly focused on preventing and treating secondary brain injuries. High pressure inside the intracranial cavity has been found to be an important feature of disturbed cerebral dynamics and secondary injuries. Thus, invasive measurement of intracranial pressure (ICP) is today a well established routine in modern neuro-intensive care. Variations in ICP can be regarded as a response of the cerebrospinal system to different stimuli, including homeostatic mechanisms which attempt to maintain the cerebral equilibrium. Nevertheless, the autoregulatory processes and their functionality may also be affected by ICP.

This study is an attempt to investigate the cerebral hemodynamics through analysis of ICP and other biomedical measurements available, such as arterial blood pressure and electrocardiography. The study is mainly conducted by analysing biomedical data through mathematical modelling, model-based frameworks, and simulations. This thesis focuses on the dynamics of intracranial pressure in either presence or absence of cerebral autoregulation. A model-based framework which describes the relationship between arterial distensibility and compliance was developed to study variations in the mechanical properties of distant cerebral artries/arteriols. The measurements of pulse wave propagation velocity as well as transfer function between arterial blood pressure and intracranial pressure were utilized as the key elements of the study. Using the aforementioned model, it was shown that variations in the level of ICP may arise from different states of cerebral autoregulation and the associated regime within the cerebral vasculature.

The state of Cerebral Blood Flow (CBF) autoregulation during plateau waves of ICP was taken as a subsequent focus of the study. The investigation was conducted by applying the mathematical models of cerebral hemodynamics to the measurements from a TBI patient. Considering the mechanical properties of the cerebrovascular system, the study examined models of impaired as well as intact CBF autoregulation as the possible options. Although the intact autoregulatory mechanism could simulate elevated ICP waves, a large time constant of regulation far from the reported response

times in human was needed. The assumption of an exhausted autoregulatory mechanism, however, led to the results pointing to a partial collapse within the cerebral arterial-arteriolar path.

Finally, the origin of plateau waves of ICP was investigated by reviewing the phenomenon from a new perspective. The estimation of the baroreceptor reflex index was utilised to locate the source of bradycardia during ICP plateau waves. The result suggested that an activation of the Cushing reflex when the cerebral arterial-arteriolar segment suffers from a partial collapse may lead to the generation of these waves. Furthermore, a negative correlation between cerebral perfusion pressure (CPP) and CBF was recognised associated to this circumstance. It is concluded that a CPP-oriented treatment of TBI patients who demonstrate ICP plateau waves may not lead to the expected regulation of CBF.

Keywords: Baroreceptor reflex, Cerebral compliance, Cerebral autoregulation, Collapsible tubes, Cushing reflex, Intracranial dynamics, Intracranial pressure, Mathematical modelling, Pulse wave propagation, Secondary brain injury, Traumatic brain injury

Acknowlegments

It is difficult to overstate my gratitude to my supervisor, Prof. Tomas McKelvey. I appreciate all his contributions of time and ideas to make my Ph.D. experience productive and stimulating. I am also thankful to former head of the Signal Processing group, Prof. Mats Viberg. It has been an honour to be a member of his research group. The joy and enthusiasm he has for his research was and will be contagious and many students will emulate it. I would also like to acknowledge Prof. Bertil Rydenhag and Catherine Eriksson Ritzèn, from Sahlgrenska Hospital University, for interesting discussions and constant support.

The members of the Signal Processing group have contributed immensely to my personal and professional time at Chalmers. I would like to express my sincere gratitude to all of them. I would also to thank the administrative and technical staff at the department of Signals and Systems. My deepest appreciation goes to many Iranian colleagues at Chalmers who became a valuable source of friendship to me.

Last, but not least, I would like to thank my family and friends for all their love and support. I am especially thankful to my father who supported me in all my pursuits. And finally, I could never express my thanks enough to my loving, encouraging, and patient husband Maziar whose faithful support during the last stage of this Ph.D. is so appreciated.

Sima Shahsavari
Chalmers University of technology
October 2011

List of Appended Papers

This thesis is based on the following papers:

Paper A S. Shahsavari, T. McKelvey, C. Eriksson-Ritzen, and B. Rydenhag. Cerebrovascular mechanical properties and slow waves of intracranial pressure in TBI patients. IEEE transactions on biomedical engineering, vol. 58, no.7, pp. 2072-82, 2011.

Paper B S. Shahsavari, T. McKelvey, C. Eriksson-Ritzen, and B. Rydenhag. A Model-Based Assessment of Cerebral Hemodynamics during Plateau Waves of ICP. Submitted to Journal of Applied Physiology, 2011.

Paper C S. Shahsavari, T. McKelvey, C. Eriksson-Ritzen, and B. Rydenhag. Plateau Waves and Baroreflex Sensitivity in Patients with Head Injury: A Case Study. In *Proceedings* of the 33rd Annual International Conference of the IEEE, Engineering in Medicine and Biology Society, 2011.

Paper D S. Shahsavari, T. McKelvey, C. Eriksson-Ritzen, and B. Rydenhag. Cushing reflex and plateau waves of intracranial pressure. Submitted to IEEE transactions on biomedical engineering, 2011.

Other related publications by the author which are not included in the thesis:

- S. Shahsavari, T. McKelvey, B. Rydenhag, and C. Eriksson-Ritzen. Pulse Wave Velocity in Patients with Severe Head Injury: A Pilot Study. In *Proceedings* of the 32nd Annual International Conference of the IEEE, Engineering in Medicine and Biology Society, pp. 5277-5281, 2010.

- S. Shahsavari, T. McKelvey, T. Skoglund, and C. Eriksson Ritzèn. A Comparison Between the Transfer Function of ABP to ICP and Compensatory Reserve Index in TBI. Presented at *13th International symposium on Intracranial and Brain Monitoring.* In G. Manley, C. Hemphill, and S. Stiver, editors, Intracranial Pressure and Brain Monitoring XIII, Acta Neurochirurgica Supplementum 102, pp. 9-13, Springer-Verlag, 2009.

- S. Shahsavari, T. Hallen, T. McKelvey, C. Eriksson-Ritzen, and B. Rydenhag. Normalized Power Transmission between ABP and ICP in TBI. In *Proceedings* of the 31st Annual International Conference of the IEEE, Engineering in Medicine and Biology Society, pp. 4699-4703, 2009.

- S. Shahsavari and T. McKelvey. Linear and Non-linear Approaches to Decomposition of Human Body Pressure Signals. Tech. report no. R005/2009, Department of Signals and Systems, Chalmers University of Technology, Göteborg, Sweden, March 2009.

- S. Shahsavari and T. McKelvey. Harmonics Tracking of Intracranial and Arterial Blood Pressure Waves. In *Proceedings* of the 30th Annual International Conference of the IEEE, Engineering in Medicine and Biology Society, pp. 2644-2647, 2008.

- S. Shahsavari and T. McKelvey. Frequency Interpretation of Tidal Peak in Intracranial Pressure Wave. In *Proceedings* of the 30th Annual International Conference of the IEEE, Engineering in Medicine and Biology Society, pp. 2689-2692, 2008.

Contents

Abstract i

Acknowledgments iii

List of Appended Papers v

Contents vii

Abbreviations and Acronyms xi

Part I: Introductory Chapters 1

1 Introduction 3

2 Traumatic Brain Injury 7
2.1 Primary Brain Damage . . . 7
2.2 Secondary Brain Damage . . . 8
2.2.1 Focal and Global Ischemia . . . 9
2.2.2 Brain Swelling . . . 10
Congestive Brain Swelling . . . 10
Cerebral Edema . . . 10
Brain Swelling in Head Injury . . . 11
2.3 Summary . . . 11

3 Physiological Background 13
3.1 Intracranial Dynamics . . . 13
3.1.1 Cerebral Compliance . . . 15
Pressure-Volume Index . . . 16
Volume-Pressure Response . . . 18
3.2 Homeostatic Mechanisms . . . 19
3.2.1 Cerebral Blood Flow Autoregulation . . . 19
Pressure-Flow Relationship in Collapsible Tubes . . . 21

Muscular Arteries . . . 22
3.2.2 Baroreceptor Reflex . . . 24
3.2.3 Cushing Reflex . . . 25
3.3 Summary . . . 25

4 Data Analysis and Modelling **27**
4.1 Intracranial Pressure Signal Analysis . . . 27
4.1.1 ICP pulse waveform . . . 28
4.2 Study of Cerebral Compliance . . . 30
4.2.1 Index of Compensatory Reserve . . . 30
4.3 Study of Cerebral Vasculature and Circulatory System . . . 32
4.3.1 Index of Cerebrovascular Pressure Reactivity . . . 33
4.3.2 Transfer Function Between ABP and ICP . . . 34
4.3.3 Pressure Pulse Wave Propagation Velocity . . . 36
Estimation of Cerebrovascular Distensibility . . . 38
4.3.4 Mathematical Modelling . . . 38
4.3.5 Study of The Baroreceptor Reflex Mechanism . . . 40
Time-Domain BRS Index . . . 40
The event technique: . . . 41
Global approach for slope estimation: . . . 41
Frequency-Domain BRS Index . . . 42
4.4 Summary . . . 43

5 Contributions **45**
5.1 Publications . . . 45

References **49**

Part II: Included Papers **59**

Paper A: Cerebrovascular Mechanical Properties and Slow Waves of Intracranial Pressure in TBI Patients **61**
Abstract . . . 63
1 Introduction . . . 63
2 Background . . . 65
2.1 Pressure Pulse Propagation . . . 65
2.2 Elastic-Muscular Arteries . . . 67
2.3 Cerebral Autoregulation - Cerebrovascular Pressure Reactivity 68
3 Methods . . . 68
3.1 Experimental Estimation of Cerebrovascular Distensibility and Compliance . . . 68
3.1.1 Data Acquisition . . . 68
3.1.2 Estimation of Cerebral Arterial Distensibility . . . 69
3.1.3 Estimation of Cerebral Arterial Compliance . . . 70
3.2 Model-Based Estimation of Cerebrovascular Distensibility and Compliance . . . 70

4 Results . . . 73
5 Discussion . . . 74
5.1 Intact Pressure Reactivity . . . 76
5.2 Impaired Pressure Reactivity-Case I . . . 77
5.3 Impaired Pressure Reactivity-Case II . . . 79
5.4 Review on Plateau Waves . . . 80
5.5 Study Limitations . . . 82
6 Conclusion . . . 82

Paper B: A Model-Based Assessment of Cerebral Hemodynamics during Plateau Waves of ICP **87**
Abstract . . . 89
1 Introduction . . . 89
2 Vascular Extensibility and Compliance . . . 90
3 Materials and Methods . . . 92
3.1 Data Acquisition . . . 92
3.2 Patient Description . . . 92
3.3 Data and Observations . . . 92
3.4 Model Description . . . 94
3.5 Assignment of Parameter Basal Values . . . 96
4 Results . . . 97
5 Discussion . . . 102
5.1 Study Limitations . . . 105
6 Conclusion . . . 105

Paper C: Plateau Waves and Baroreflex Sensitivity in Patients with Head Injury: A Case Study **109**
Abstract . . . 111
1 Introduction . . . 111
2 Materials and Methods . . . 112
2.1 Experimental Data . . . 112
2.1.1 TBI Data . . . 112
2.1.2 EuroBaVar Data Set . . . 113
2.2 Methods . . . 113
2.2.1 Time-Domain BRS Index . . . 113
2.2.2 Frequency-Domain BRS Index . . . 114
3 Results . . . 115
4 Discussion and Conclusions . . . 116

Paper D: Cushing Reflex and Plateau Waves of Intracranial Pressure **121**
Abstract . . . 123
1 Introduction . . . 123
2 Background . . . 124
2.1 Plateau Waves . . . 124
2.2 Baroreceptor Reflex . . . 125
2.3 Cushing Reflex . . . 125

3 Materials and Methods 126
3.1 Experimental Data 126
3.2 Methods 128
3.2.1 Time-Domain BRS Index 128
3.2.2 Frequency-Domain BRS Index 129
3.2.3 Heart Rate Variability 129
4 Results 129
5 Discussion 130
6 Conclusions 134

Abbreviations and Acronyms

ABP	Arterial Blood Pressure
AMP	Amplitude of the fundamental cardiac component in the ICP waveform
C	Compliance
CBF	Cerebral Blood Flow
CBR	Cerebrovascular Resistance
CPP	Cerebral Perfusion Pressure
CSF	Cerebrospinal Fluid
CT	Computed Tomography
DAI	Diffuse Axonal Injury
DVI	Diffuse Vascular Injury
FFT	Fast Fourier Transform
ICP	Intracranial Pressure
ICP_{mean}	Mean Intracranial Pressure
JVP	Jugular Venous Pressure
P	Pressure
PRx	Pressure Reactivity Index
PVI	Pressure-Volume Index
RAP	Correlation coefficient between the amplitude of the fundamental component and mean intracranial pressure
TBI	Traumatic Brain Injury
V	Volume
VPR	Volume-Pressure Response
BBB	Blood-Brain Barrier

Part I

Introductory Chapters

CHAPTER 1

Introduction

> Do not go where the path may lead,
> go instead where there is no path and
> leave a trail.
>
> Ralph Waldo Emerson

Traumatic Brain Injury (TBI) is a major cause of death and permanent disability worldwide. Despite a rapid growth in both active and passive safety technologies, fatalities from head injury, caused by motor vehicle accidents, are increasing. Statistics reveal more mortalities in developing countries compared to developed countries and among the young population compared to the old population. Moreover, penetrating brain injury, resulting from urban violence and armed conflict, is still an increasing problem in many communities. Work and sport accidents which may lead to TBI injuries, should not be ignored [1].

In the 1950's, over 80% of patients with severe brain injuries died as a result of their injuries. In the twenty first century, mortality rates around 25% are commonly reported [1]. In 1999 approximately 5.3 million American were living with TBI-related disabilities [2]. Based on a report issued in 2006 by U. S. Centers for Disease Control and Prevention, each year 1.4 million people in the United States will sustain a TBI. Of this number 50,000 die, 235,000 are hospitalized and 1.1 million are treated and released from an emergency department [3].

Figure 1.1 represents a comparison between incidence of TBI and other leading injuries and diseases carried out by the Brain Injury Association of America [4]. The results show that TBI is responsible for approximately 86% of injuries. TBI statistics may vary due to different data sources and nomenclatures. This means they may include or exclude such categories as minor head injuries, skull fractures, and non-hospitalised TBI survivors. Despite a lack of accurate statistics, the above

information pinpoints the crucial role of treatment schemes for TBI patients and technologies involved.

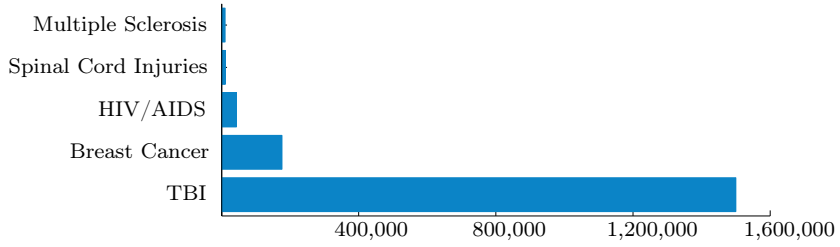

Figure 1.1: A Comparison between incidences of traumatic brain injury and other leading injuries or diseases. Data from [4].

The primary aim in the neurointensive care of TBI patients is to prevent and treat secondary brain injury. This requires cerebral perfusion pressure (CPP) to be maintained in a normal range in order to meet the brain's metabolic demands for oxygen and glucose. Raised intracranial pressure (ICP) can disrupt cerebral perfusion. High ICP has been found to be an important cause of secondary brain injury, associated with ischemia, brain herniation, and poor outcome after brain injury. Hence, ICP monitoring has become a well-established discipline of brain monitoring after traumatic brain injury in almost all neurointensive care units.

Today, the time average of the ICP signal is usually used in clinical practices to evaluate the dynamic state of the brain and to guide ICP or CPP-oriented protocols [5]. However, many researchers have faith in more valuable information, which is hidden in ICP. The information is correlated to cerebral hemodynamics and can be used for early detection and treatment of secondary injuries. Various investigations have been performed based on this shared sentiment, and many still are ongoing. Although these investigations might seem diverse in approach, they are in essence unique, as they all aim to extract features of cerebral dynamics from measured intracranial pressure.

This study is an attempt to investigate the cerebral hemodynamics and involved autoregulatory mechanisms including cerebral blood autoregulation and the Cushing reflex. The investigation is conducted through a model-based framework. The major aim is to use ICP in combination with other available biomedical signals to track the changes in the cerebrospinal territory. This information is then used to provide a clearer map of the interaction between different regulatory mechanisms as well as a better understanding of cerebral events such as ICP plateau waves.

Research Project

The research project is a joint collaboration between Signal processing group at Chalmers University of Technology and Sahlgrenska Hospital University.

Outline of the Thesis

The thesis is divided into two parts. The first part gives an introduction and provides the background needed to those not familiar with the subject. The second part includes the author's contribution in the form of appended papers. The outline of the first part is as follows. Chapter 2 gives an overview on pathophysiological aspects of traumatic brain injury. Phenomena such as swelling, brain edema and ischemia are introduced. Chapter 3 provides background information on intracranial dynamics. Signal analysis of the intracranial pressure is addressed in Chapter 4. Finally, Chapter 5 is dedicated to the contribution made by this thesis.

CHAPTER 2

Traumatic Brain Injury

Act as if what you do makes a difference. It does.

William James

The complex anatomic and physiologic abnormalities of traumatic brain injury are initiated by different procedures. To name a few, it can include a blow to the cranium, rapid acceleration/deceleration and rotation of the brain when it is forcefully moved back and forth against the bony structures inside the skull. The properties of the intracranial components, whether fluid or solid, soft or hard, predispose the brain to certain types of injury [6]. Deaths from head injury comprise 1-2 per cent of all deaths from all causes and between 25-50 per cent of all deaths from trauma. 1-5 per cent remain vegetative and 5-18 per cent are severely disabled six months after their injury [7]. Falls, motor vehicle accidents and assaults are among leading causes of traumatic brain injury. Traumatic brain injury is a broad term that describes a vast array of damage to the brain, including primary and secondary types of brain damage.

2.1 Primary Brain Damage

Primary brain damage refers to a sudden and profound brain tissue deformation that is considered to be more or less complete immediately after the time of the impact. This occurs at the exact time of accident such as car accident, gunshot wound, or a fall. These deformations might directly damage the blood vessels, axons, neurons, and glia in a focal, multifocal, or diffuse pattern of involvement. This will also result in dynamic and evolving processes depending on the anatomical site of the injury. Table 2.1 provides a list of primary brain damages [7].

Table 2.1: Primary traumatic brain damage (neural and/or vascular)

Diffuse
1. Diffuse axonal injury (DAI)[1]
2. Diffuse vascular injury (DVI)[2]

Focal
1. Vascular injury resulting in:
   (a) Intracranial haemorrhage
   (b) Subdural haemorrhage
   (c) Epidural haemorrhage (extradural haemorrhage)
   (d) Subarachnoid haemorrhage

2. Axonal injury
3. Contusion[3]
4. Laceration[4]

2.2 Secondary Brain Damage

As described in the previous section, trauma to the brain causes a variety of primary injuries by means of the mechanical disruption of brain tissue and vasculature. TBI also causes cellular, chemical, tissue, or blood vessel changes in the brain that develop over a period of hours or days after the initial traumatic insult and contribute to further destruction of brain tissue [8]. These changes include cellular depolarisation, cell membrane dysfunction with disturbance of ion homeostasis, excessive release of excitatory amino acids, free radical production, mitochondrial damage, vascular damage, disruption of the blood-brain barrier (BBB), inflammation, impaired cerebrovascular autoregulation, hematoma, edema formation, and increased pressure inside of the skull (intracranial pressure).

A cascade of secondary events may cause a secondary brain injury in addition to the initial damage [9]. In any given patient, there may be a complex and dynamic interplay of the different primary and secondary types of brain damage. This can produce a unique constellation of lesions both in terms of anatomical site and quantity. For example, the consequences of primary vascular damage may be bleeding into brain tissues to produce an intracerebral hematoma or interference in brain perfusion with resultant ischemic damage (secondary brain damage), or a combination of both. Thus, head injury is not a single entity but consists of many different types of lesions that

[1] Nerve impulses leave nerve cells through a part of the nerve cell called the axon. In diffuse axonal injury, axons throughout the brain are damaged

[2] DVI is seen in patients who die very soon after head injury and consists of multiple small haemorrhages throughout the brain [7]

[3] Complex dynamic evolving time dependent neural tissue injury which often occurs right under the location of impact or at points where the force of the blow has driven the brain against the bony ridges inside the skull and involves a complex interplay of vascular, glial, neuronal injury plus secondary edema and ischemia

[4] Tearing of the frontal (front) and temporal (on the side) lobes or blood vessels of the brain (the force of the blow causes the brain to rotate across the hard ridges of the skull, causing the tears)

might occur rarely in isolation, or more commonly in varied combinations. A list of secondary brain damages is represented by Table 2.2 [7].

Table 2.2: Secondary brain damage

Diffuse
1. Diffuse hypoxic-ischemic damage
2. Diffuse brain swelling
Focal
1. Focal hypoxic-ischemic damage
2. Focal brain swelling

2.2.1 Focal and Global Ischemia

Cerebral Blood Flow (CBF) in an uncollapsed cerebral vasculature is derived using the net pressure gradient, the so-called cerebral perfusion pressure (CPP). The relationship between CBF and CPP can be described thus:

$$CBF = CPP/CBR, \tag{2.1}$$

where CBR denotes cerebrovascular resistance. Altered CBF as a consequence of vascular injury can lead to a reduced or absent perfusion of brain tissues in the territory of the affected blood vessel(s) and in case of inadequate collateral circulation may result in focal or regional ischemia[5]. Global ischemia (non-perfused brain), on the other hand, occurs when CPP drops below a critical threshold (in practice 45 mmHg) [7]. CPP is usually defined as the pressure difference between the arterial side and venous side thus:

$$CPP = mean(ABP) - mean(JVP), \tag{2.2}$$

where ABP and JVP stand for arterial blood pressure and jugular venous pressure, respectively. However, a third pressure exists which contributes to cerebral perfusion pressure. Intracranial pressure is an external pressure to the blood vessels which at high levels can restrict flow through the tissues. According to the starling resistor mechanism, a primary increase in ICP provokes a collapse or narrowing of the terminal intracranial veins, which in turn, causes pressure in the upstream large cerebral veins to rise to ICP [10]. In this condition, CBF depends on the difference between ABP and ICP through

$$CPP = mean(ABP) - mean(ICP); \tag{2.3}$$

therefore, global ischemia can result from either an increase in ICP or a decrease in ABP. The ischemic brain damage tends to be focal, but if elevated ICP is unrelieved,

[5]A reduction of CBF is often seen in the early hours after severe head injury

leading to reduced CPP, then global ischemic brain damage may occur. This may result in wide-ranging types of tissue damage from selective neuronal necrosis[6] to infarction[7] [7].

2.2.2 Brain Swelling

Partial or general brain swelling may occur after head injury due to increased intravascular blood volume, increased tissue water content of the brain, or a combination of both. The former type of swelling is called *congestive brain swelling* while the latter has been named *cerebral edema* [7]. Swelling of the brain becomes dangerous when it causes a rise in intracranial pressure which prevents blood from entering the skull and delivering glucose and oxygen to the brain. Swelling can also block other fluids from leaving brain, making the swelling even worse. Treatment of brain swelling can be difficult. A structured protocol for medication and surgical procedures is beneficial.

Congestive Brain Swelling

Arterial dilatation and/or venous obstruction followed by increased cerebral blood volume may lead to congestive brain swelling. Congestive brain swelling may rapidly occur in patients, particularly in children. Massive cerebral hemisphere swelling, 20 minutes after head injury, has been documented by Computed Tomography (CT) [7].

Cerebral Edema

By definition, cerebral edema is the extracellular accumulation of fluid in the brain tissue and, counts as an important secondary response to trauma. Edema can be classified into five different categories:

- *Vasogenic edema* is the accumulation of protein-rich fluid in the extracellular space (hypodense white matter on CT) and occurs due to BBB impairment. The localized swelling related to contusions and intracranial hematoma is an example of vasogenic edema.
- *Cytotoxic edema* or intracellular swelling occurs in association with hypoxic-ischemic damage where a disturbance of ionic gradients leads to the accumulation of intracellular fluid (hypodense white and grey matter on CT).
- *Hydrostatic edema* refers to the extracellular accumulation of protein-poor fluid in an intact vascular bed arising from a sudden increase in intravascular or transmural pressure. Hydrostatic edema might follow a sudden decompression of a mass lesion or happen due to defective autoregulation.
- *Osmotic brain edema* addresses increased intracellular water resulting from a critical reduction in serum osmolality.

[6] Necrosis is the name given to premature or unnatural death of cells and living tissue

[7] The formation of an area of necrosis in the brain, including the cerebral hemispheres (cerebral infarction), thalami, basal ganglia, brain stem (brain stem infarctions), or cerebellum secondary to an insufficiency of arterial or venous blood flow

- *Interstitial brain edema* refers to the condition in which a high pressure obstructive hydrocephalus results in a periventricular extravasation of water. This is, however, an uncommon event in head injury [7].

The causes and consequences of cerebral edema are poorly understood.

Brain Swelling in Head Injury

Brain swelling resulted from head injury can be classified into three main categories:

- *Swelling around cerebral contusions and intracerebral haemorrhages* is a consequence of a diverse combination of vascular damages and may lead to BBB disruption. The swelling is usually followed by vasogenic edema and ischemic damage resulting in cytotoxic edema.
- *Diffuse swelling of one cerebral hemisphere* refers to a massive cerebral swelling which is not related to contusions, intracerebral haemorrhage or focal infarction. Because of the quick nature, the swelling is classified as a congestive swelling. Nevertheless, the subsequent ICP increase may also result in cytotoxic edema.
- *Diffuse cerebral swelling of the entire brain* has been reported more frequently among children rather than adults. The pathogenesis of diffuse brain swelling is unclear [7].

2.3 Summary

Most secondary injuries arise during the first 12-24 hours after a trauma, but it might happen at any time during the first 5-10 days in patients with very severe primary brain injury [8]. Different types of secondary brain damages are potentially reversible by help of early diagnosis and adequate treatment. Physicians cannot treat primary brain injuries; predicting and decreasing secondary injuries can, however, help them to prevent further brain damage. Identification and measurement of secondary brain injuries have, hence, attracted considerable interest as key elements in the treatment of TBI patients. These issues will be discussed in the next chapters.

CHAPTER 3

Physiological Background

> It's not what you look at that matters, it's what you see.
>
> Henry David Thoreau

Edema, swelling, ischemia, and other mechanical, physical, and biochemical disturbances of the brain can rarely be measured by direct procedures. This necessitates the identification of some quantifiable parameters. These parameters should be highly correlated with desired brain functions, even though they are not the direct measurement of the underlying mechanisms. To achieve this goal, understanding of intracranial dynamics and related homeostatic mechanisms is of great importance.

3.1 Intracranial Dynamics

The classical Monro-Kellie doctrine [11, 12] was the first step to describe intracranial hemodynamics. It proposed that the brain and its contained blood are incompressible, confined within the nearly rigid skull, the total volume of which remains constant. Later, cerebrospinal fluid (CSF)[8] was taken into account as another cranial compartment when the concept of reciprocal volume changes between blood and CSF was introduced by Burrows [13]. Within an intact skull, the total volume is controlled at a relatively fixed level by various homeostatic mechanisms. An increase in volume in any single compartment of the skull, therefore, creates a pressure gradient in the other compartments. This simply means that an increase in one of these compartments causes a reduction in one or both of the remaining two [9, 14].

[8] The clear, water-like fluid that occupies the cerebral space and central canal of the spinal cord and cushions the brain and spinal cord

As Figure 3.1 shows, the brain parenchyma occupies 80-85 per cent of the total intracranial volume (1200-1600 cc.) The remaining space is filled with blood (100-150 cc) and CSF (100-150 cc). Blood and CSF, which form around 20 per cent of the intracranial volume, are capable of rapid extracranial displacement. The fluid content of the brain parenchyma, intra- and extracellular fluid, may also change due to pathological conditions or medical treatments. These four fluid volumes have the key role in preserving the volume equilibrium of the intracranial space [15].

Elevated ICP results from an increase in the volume of the intracranial contents. Any disturbance in the intracranial volume equilibrium disrupts ICP equilibrium so that the magnitude of the ICP change will depend on the magnitude and rate of the volume interchange as well as the varying compliance of each intracranial compartment. In general, ICP changes can be divided into two categories with vascular and nonvascular origin. The nonvascular mechanism, which represents increase in brain bulk, can be due to:

- *edema*
- *increased intracerebral, extradural, or subdural mass lesion*
- *increased CSF outflow resistance*[9]

Vascular mechanisms include:

- *active cerebral vasodilatation* that is caused by physiological stimuli such as increased level of carbon dioxide or decreased arterial inflow pressure in the case of intact pressure autoregulation
- *passive distention of cerebral vessels* in the absence of autoregulation
- *venus outflow obstruction*

As mentioned in the previous chapter, both cerebral edema and congestive brain swelling can be recognised as the possible cause of an increased ICP, the former as a nonvascular and the latter as a vascular mechanism. Owing to the connection between the ICP level and cerebral events, over the past decades ICP has been found to be a qualified candidate to study the brain state. In the 1950s, the first ventricular ICP monitor was introduced by Nihls Lundberg [16]. The device consisted of a Silastic catheter inserted into the lateral ventricle and connected to an external transducer via a fluid-filled column. Using this device and by the continuous monitoring of ICP, Lundberg found TBI associated with elevated ICP and identified several therapies including hyperventilation which aim at reducing ICP [17].

ICP variations may have a significant impact on outcomes after TBI. Sustained ICP, greater than 20-25 mmHg, has been found to be associated with poorer outcomes from injury [18–20]. The higher rate of mortality and morbidity is reported for high levels of ICP (particularly the peak ICP level) [20–23]. Several studies point out the existence of strict relationships between ICP changes and brain hemodynamic perturbations [24–27]. Therefore, the analysis of ICP time patterns in order to provide a quantitative description on intracranial dynamics has become of great clinical value.

[9] Hydrocephalus

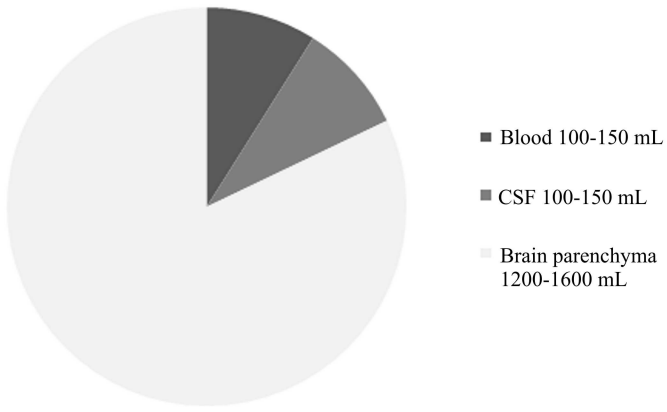

Figure 3.1: The major intracranial contents by volume. CSF and ECF stand for cerebrospinal fluid and extracellular fluid respectively. Data from [1].

ICP is formed by a non-linear dynamic process with high complexity in relationships among physiological quantities. At the present time, various physiological and pathophysiological factors influencing ICP are not fully understood, and many approaches to study ICP are found inadequate to grasp important aspects of intracranial dynamics. As a result, hidden information in the ICP signal is insufficiently utilized in the clinical setting [10].

3.1.1 Cerebral Compliance

Although the Monro-Kellie doctrine pointed out the existence of a connection between fluctuations in intracranial volume and the consequent intracranial pressure gradient, it did not reveal any further information about this dynamic relation. Ryder *et al.* [28] was the first to introduce a non-linear (hyperbolic) craniospinal pressure-volume curve (see Figure 3.2). The slope of the intracranial volume-pressure curve (right plot in Figure 3.2), which correlates to the viscoelastic properties of the brain, skull, and dural, is known as cerebral compliance and defined by

$$C = \triangle V / \triangle P, \tag{3.1}$$

where $\triangle V$ is the change in volume, and $\triangle P$ represents the change in pressure. Cerebral compliance simply represents the capacity of the intracranial space to accommodate extra volume. The horizontal phase in the craniospinal pressure-volume curve, which can be recognized in the left bottom corner of the left plot, represents the phase when blood and CSF can be readily displaced into the extracranial venous system and spinal subarachnoid space, respectively. By this, the increase in another volume or addition of a new volume can be compensated without any rise in ICP. However, when the volume continues to increase, the rate of ICP increment speeds up dramatically due to an increased need for blood and CSF displacement. Figure 3.3 shows the re-

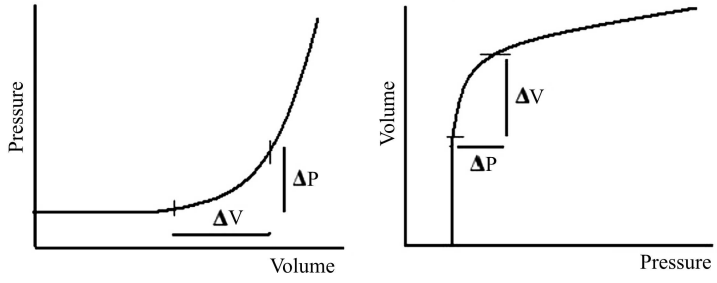

Figure 3.2: Intracranial pressure-volume relationship or elastance (left) and volume-pressure relationship or compliance (right)

quired force versus the displaced volume of CSF, venous, and arterial blood volumes. Cerebral compliance is determined by the interaction of the compliances of vascular and CSF compartments. Hence, the pressure-volume curve can be regarded as the summary of all these tree curves [15].

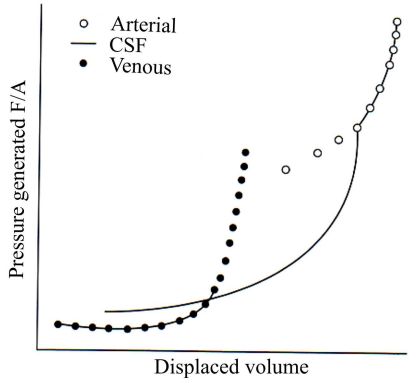

Figure 3.3: The contribution of CSF, venous, and arterial blood volume displacement to the pressure-volume curve. Pressure is defined here as the required force to displace the compensating fluid. Reproduced with permission from [15].

Pressure-Volume Index

The concept of the pressure-volume relation was developed further, when the pressure-volume relationship was mathematically modelled as a mono-exponential function by Marmarou in 1973 [29]. The model can be presented as

$$P_P = P_0 10^{\lambda V}, \tag{3.2}$$

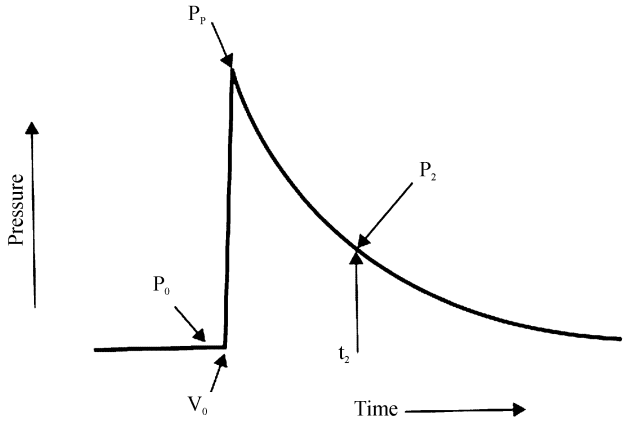

Figure 3.4: Intracranial response to bolus injection. P_0 is the baseline pressure, P_P the maximal pressure resulting from a bolus volume injection V and P_2 refers to the pressure point on the return trajectory at time t_2 (usually selected at 2 minutes post-injection). Reproduced with permission from [15].

where P_0 is the baseline pressure, and P_P represents the maximum pressure resulting from a bolus volume injection V into the cerebrospinal space (see Figure 3.4). As a corollary from this study, Marmarou demonstrated that the non-linear craniospinal pressure-volume relationship is linearized by relating the logarithm of pressure to volume. The slope of this new relationship is called pressure-volume index PVI and is formulated as

$$PVI = \frac{V}{\log(P_P/P_0)} = \frac{1}{\lambda}. \tag{3.3}$$

The PVI index, which represents the volume required to raise ICP tenfold, can be obtained from the pressure change induced by a rapid injection or withdrawal of CSF into or from cerebrospinal space. Taking the derivative of (3.2) leads to

$$\begin{aligned} \frac{dP}{dV} &= P_0 10^{\lambda V} \ln(10)\lambda \\ &= \ln(10)\frac{P}{PVI}, \end{aligned} \tag{3.4}$$

which leads to a relation between PVI and compliance thus:

$$C = \frac{dV}{dP} = 0.4343\frac{PVI}{P}. \tag{3.5}$$

As shown by (3.5), compliance has direct relationship with PVI. Thus, Marmarou concluded that the terms PVI and C can be used interchangeably [30].

Volume-Pressure Response

At approximately the same time as Marmarou, Miller *et al.* [22, 31] used a similar methodology and defined the volume-pressure response by

$$VPR = (P_P - P_0)/V \approx \frac{1}{C}, \tag{3.6}$$

which is another evaluation of craniospinal volume-pressure relationship. Here, P_0 is the baseline pressure, and P_P refers to the maximal pressure resulting from a bolus volume injection V (see Figure 3.4). The VPR technique was superior in the sense of simplicity and being independent of the assumption of mono-exponential pressure-volume relationship. Miller emphasised that if there were only one single volume-pressure curve, the absolute ICP alone would be adequate to determine the state of a patient's cerebrospinal system, and no further information would be gained by measuring compliance. However, in patients with head injuries, the degree of brain midline shift observed in CT scan correlated better to the VPR than it did to absolute ICP [32]. In 1975, Miller *et al.* [33–35] showed that the shape of the volume-pressure curve not only varies from one subject to another subject, but also is unlike for one patient under different circumstances and at different times. This can be observed in Figure 3.5.

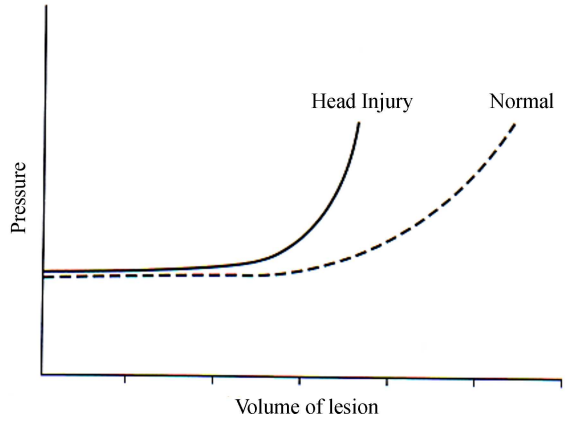

Figure 3.5: Following a head injury, the shape of pressure-volume curve may be altered such that the "break point" is shifted to the left due to a reduced buffering capacity. Adopted with permission from [15].

There is no doubt that any information about a patient's craniospinal pressure-volume relationship can be more informative than measured ICP in predicting the intracranial state. However, applying PVI or VPR technique involves some drawbacks which restrict them from being routinely used in neurosurgical practices. First, with these techniques there is an increased risk of infection that is a particular complication of ventriculostomy related to the duration of monitoring. The second disadvantage is a risk of provoking an insult to the traumatized brain and, consequently, developing a

secondary brain injury due to a rapid volume injection and activation of secondary vasodilatation. The third concerns the variability of measurements caused by inevitable changes in injection speed which often requires the repetition of measurements [32]. The aforementioned drawbacks opened the door to less invasive methods including ICP waveform analysis [36–39], which will be introduced in the next chapter.

3.2 Homeostatic Mechanisms

Homeostasis is the maintenance of equilibrium, or constant conditions, in a biological system by means of automatic mechanisms that counteract influences tending toward disequilibrium. The development of the concept, which is one of the most fundamental in modern biology, began in the 19th century when the French physiologist Claude Bernard noted the constancy of chemical composition and physical properties of blood and other body fluids. The term homeostasis was coined by the 20th-century American physiologist Walter Bradford Cannon, who refined and extended the concept of self-regulating mechanisms in living systems [40].

The human body consists of trillions of cells all working together for the maintenance of the entire organism. Despite the difference in their biological role, all cells are similar in their metabolic requirements. All need enough oxygen, glucose, mineral irons, hormones, organic and inorganic substances, and waste removal to survive and function. This necessitates the internal environment of the body to be maintained constant through some regulatory mechanisms. The processes by which the body regulates its internal environment are referred to as homeostatic mechanisms. Homeostatic mechanisms involve constant monitoring and regulating of numerous factors. The level of these factors in body fluid remains unchanged, within limits, in spite of changes to the external environment.

Systemic blood circulation, the major part of a circulatory system, supplies oxygen and nourishment to all tissues in the body except the heart and lungs and removes their waste products. A maintained equilibrium in the body is not, therefore, feasible without regulation of the systemic circulation. The complex regulation of the systemic circulatory system, which is made up of the heart and vessels, is performed using different homeostatic mechanisms. Among other cardiovascular regulatory processes, cerebral blood flow autoregulation, the baroreceptor reflex, and the Cushing reflex can affect the cerebral equilibrium on account of their counteraction with the systemic circulatory system and, hence, are found relevant to the topic of this thesis.

3.2.1 Cerebral Blood Flow Autoregulation

Even though cerebral compliance is one of the fundamental properties of the cerebrospinal system, cerebral dynamic is not fully understood without taking cerebral blood flow autoregulation into account. Interaction between these two mechanisms is of great interest in systematic approaches to identify the intracranial state. The block diagram in Figure 3.6 is the summary of intracranial dynamics which was modelled mathematically by Ursino *et al.* [10] in 1997. This model includes both cerebral compliance and cerebral autoregulation as the fundamental components and consists

of three negative feedback loops with the tendency to stabilizing ICP. As described earlier, any increase in ICP causes a parallel increase in cerebral venous pressure, hence, a decrease in both CPP and CBF. Decrease in CBF, in turn, triggers the autoregulation mechanism and causes a vasodilation which leads to increase in CBV and ICP (see loop IV). This closed system needs to modify venous outflow to compensate for the arterial inflow volume perturbation. In a normally perfused brain, arterial vasodilation moves the CSF surrounding basal arteries to bridge veins as a hydraulic piston and to compress the distal collapsible part of veins. As a result, an amount of blood exactly equivalent to arterial volume displacement associated to the cerebral blood inflow is pressed out from the intracranial system. Another mechanism to compensate the increases in intracranial volume can take place through displacement of CSF into the spinal subarachnoid space. By this, both intracranial volume and pressure consequently drop to the normal level again (see loop I). In a brain with dysfunctional mechanisms, this cascade of events, the so-called vasodilatory cascade, can continue until vasodilation is at a maximum [10, 14].

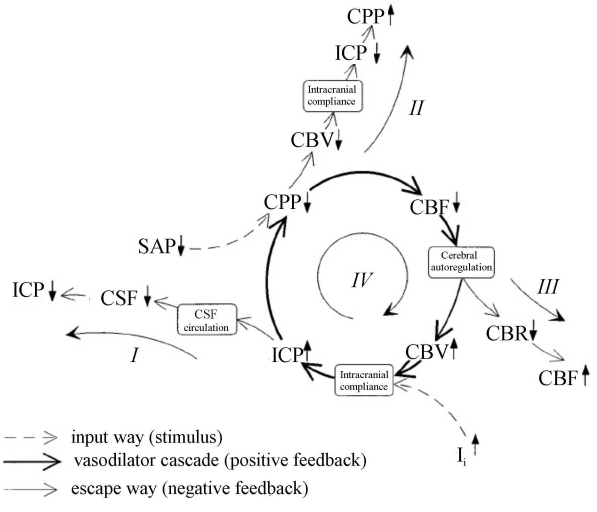

Figure 3.6: A model of intracranial dynamics proposed by Ursino *et. al.* [10]. CBV, cerebral blood volume; CSFV, cerebrospinal fluid volume; SAP, systemic arterial pressure. Adopted from [10].

Autoregulation is an indication of local blood flow regulation. The mechanism for autoregulation has been suggested to be a combination of a number of factors, including mechanical (transmural pressure or myogenic regulation) and chemical (metabolic autoregulation) aspects. The myogenic autoregulation of blood flow describes the vascular reflexes that attempt to maintain a near constant blood flow over the wide ranges of perfusion pressure [41]. Cerebral myogenic autoregulation or simply cerebral autoregulation is a physiological protective mechanism that prevents brain ischemia during blood pressure decrease and capillary damage and edema formation during blood pressure increase. Different organs display a varying degree of autoregulation. Among them, cerebral circulation shows one of the most excellent autoregulatory

behaviours. This protective mechanism can, however, be ceased after a head injury and may cause unfavourable outcomes associated with secondary insults [42–44]. To better understand the cerebral autoregulation of blood flow, we need a short overview on pressure-flow relationship in blood vessels.

Pressure-Flow Relationship in Collapsible Tubes

The study of pressure-flow relationship in vessels transporting fluids and blood to various sites of the body of living beings is one of physiologists' most difficult issues. A great deal of attention in fluid mechanics has been given to the pressure-flow relationship in collapsible tubes. Since vessels in living body are usually exposed to collapse when their internal pressure is not enough to overcome the external force, the pressure-flow relationship in collapsible tubes has found numerous physiological and medical application [45].

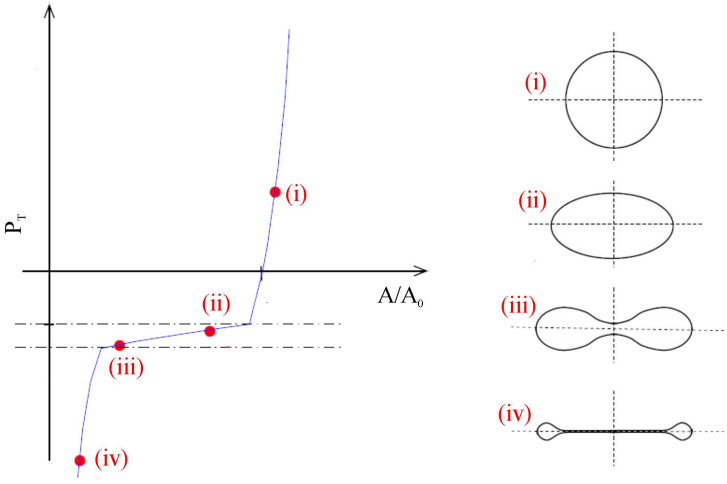

Figure 3.7: Left: Schematic representation of the tube law. Right: typical tube shapes. Reproduced with permission from [46]

Any elastic tube will collapse when the surrounding radial force is of sufficient magnitude to deform its wall. This means for a large pressure outside the tube, the cross-section of the tube does not remain circular, but flattens to an elliptical configuration, as shown in (i)-(ii) in Figure 3.7. This is the initial point of the partial collapse phase. With a further decrease in the transmural pressure P_T, the tube buckles non-axisymmetrically, typically to a two-lobed state. Once buckled, only the tube's small bending stiffness resists any further collapse. Hence, the tube undergoes a large variation in cross-sectional area when P_T changes slightly; see (ii)-(iii) in Figure 3.7. As the external force increases the opposite walls of the tube come into contact, and the tube fully collapses; (iv) in Figure 3.7. As illustrated in the figure, deforming the tube from (iii) to (ii) and, consequently, to (i) only requires a small

increase in the pressure inside the tube. Therefore, this region is called the region of "*free distensibility*". Once the tube becomes inflated, an increase of considerable magnitude is needed in the tube internal pressure to produce further radial stretch and hence volume.

The above description simply creates the expectation of a nonlinear pressure-flow relationship in collapsible tubes. Figure 3.8 demonstrates a typical pressure-flow curve for a collapsible elastic tube. In this figure, ΔP and Q refer to the pressure drop across and volumetric flow rate within the collapsible tube. Different parts of the curve are labelled to indicate the regime associated with them. As show, in an uncollapsed phase, vessel deformation remains very small, and the relation between Q and $\triangle P$ is essentially direct and linear. Within this phase, the flow can be described by the Poiseuille equation thus:

$$Q = \frac{\pi r^4 \Delta P}{8\mu L}, \tag{3.7}$$

where μ is the dynamic viscosity of the liquid, and r stands for the internal radius of the tube [47]. The term $8\mu L/\pi r^4$ in (3.7) can be regarded as the resistance of the tube to the flow. From Figure 3.8 an uncollapsed elastic tube can be found exposed to a passive extension when ΔP increases, the consequences of which is an augmentation in fluid flow according to (3.7).

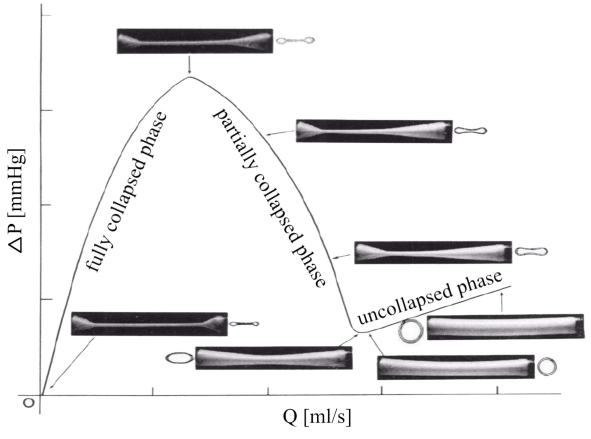

Figure 3.8: A typical pressure-flow curve for a collapsible tube. $\triangle P$ is the pressure drop across and Q is the volumetric flow rate within the collapsible tube. Transverse and longitudinal cross-sections of the tube are shown for various $\triangle P - Q$ states. Reproduced with permission from [48]

Muscular Arteries

The aforementioned discussion concerns with the elastic properties of vessels; nevertheless, a full interpretation of the behaviour of arterial walls necessitates an overview of the composition of their materials. In general, the blood vessels of the human body

can be classified into two major categories: elastic and muscular vessels. The elastic materials of the former class are mainly collagen and elastin. Smooth muscle is another major constituent of the arterial wall in muscular vessels. Despite its contribution to the tension in the wall, a smooth muscle cannot properly be regarded as a true elastic material. Smooth muscle cells exhibit a predominantly circumferential orientation, and therefore their contraction is mainly in circumferential direction. These cells are excited by an increase in arterial pressure to produce a contractile tension which is capable of decreasing the diameter of the artery by 20-50 per cent [47]. The pressure-dependent activation of the smooth muscle in the resistant part of the circulatory system (small arteries and arterioles) is the underlying physiological mechanism behind the blood flow autoregulation. From (3.7), CBF is equal to CPP divided by CPR. Hence, cerebral blood flow can be regulated by the excitation of the smooth muscle resulting in vasodilation when blood pressure falls and vasoconstriction when the pressure rises.

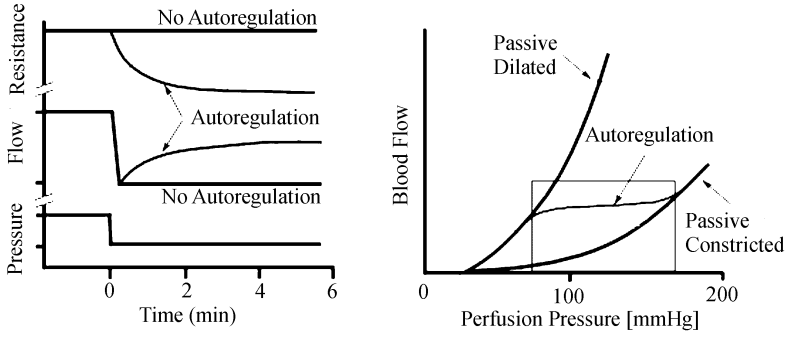

Figure 3.9: Autoregulatory response. Top plot: When perfusion pressure falls from 100 to 70 mmHg, flow soon decreases by approximately 30%. If the organ is capable of autoregulation, flow returns back to the control in few minutes as a result of reduction in arterial resistance (lines marked with *Autoregulation*). Otherwise, in the case of an impaired autoregulatory mechanism, the flow will remain low. Bottom plot: The line marked with *Autoregulation* represents the autoregulatory range in which flow remains relatively constant despite the changes in perfusion pressure. Passive dilated/constricted curves refer to an impaired autoregulatory mechanism resulted from a maximally dilated/constricted vasculature, where flow passively follows the changes in perfusion pressure. Reproduced with permission from [42].

Figure 3.9 demonstrates an example of the autoregulatory response in the left-hand plot. When perfusion pressure falls from 100 to 70 mmHg, flow quickly decreases by approximately 30 per cent. If the organ is capable of autoregulation, flow returns back to the control in a few minutes as a result of reduction in arterial resistance (lines marked with *Autoregulation*). Otherwise, in case of an impaired autoregulatory mechanism, flow will remain low. The right plot shows the relationship between steady-state flow and perfusion pressure. The line marked with *Autoregulation* represents the autoregulatory range in which flow remains relatively constant despite the changes in perfusion pressure. Passive dilated/constricted curves refer to an impaired autoregulatory mechanism resulted from a maximally dilated/constricted vasculature,

where flow passively follows the changes in perfusion pressure. As the figure shows, a region exists with the lower and upper pressure limits. Beyond these limits, an organ is not capable of autoregulation.

3.2.2 Baroreceptor Reflex

Cardiovascular activity is regulated by intrinsic rhythmicity of the myocardium as well as various local reflexive mechanisms. Among different regulatory pathways from the brain, the baroreceptor reflex is a homeostatic mechanism that maintains blood pressure of the human body through the central nervous system [49]. Autonomic control of the heart rate and systemic blood pressure are completed through parasympathetic (vagus) and sympathetic (cardioaccelerator) neural activities. Parasympathetic stimulation leads to a lower heart rate, followed by a decline in both cardiac output and blood pressure. The sympathetic branch of the autonomic nervous system, however, acts upon three different levels and has opposing effects on the blood pressure. Sympathetic activation increases the heart rate as well as the contractile strength of the heart, resulting in increased cardiac output and blood pressure. It also affects the circulatory system on the arterioles and veins level, by means of vasoconstriction. The latter leads to an elevation in blood pressure associated with increased total peripheral resistance (TPR) and venous return.

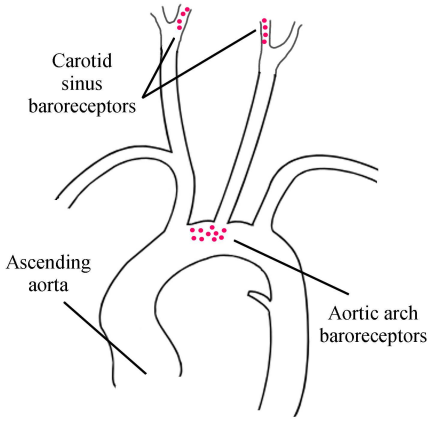

Figure 3.10: Stretch-sensitive baroreceptors, located on the carotid sinuses and aortic arch activate the baroreceptor reflex mechanism through stimulation of sympathetic or parasympathetic branches of the neural system.

When systemic blood pressure increases, the baroreceptor reflex generates a negative feedback which decreases the heart rate as well as blood pressure. The feedback is initiated on the level of stretch-sensitive baroreceptors located on the carotid sinuses and aortic arch (see Figure 3.10), and acts through the inhibition of the sympathetic and activation of the parasympathetic nervous system. Conversely, a decrease in arterial blood pressure increases sympathetic neural activity and decreases the neural activity of the parasympathetic branch, resulting in an increase in heart rate, stroke

volume, and total peripheral resistance. By this, arterial blood pressure will return to its normal level [49]. The summary of the neural system effects upon the circulatory system is provided by the block diagram in Figure 3.11.

3.2.3 Cushing Reflex

A systemic hypertension following an elevated intracranial pressure was first reported by Cushing in 1901 [50]. The phenomenon is called the Cushing reflex, but it is also referred to as vasopressor response. There is no universal agreement on the possible mechanisms behind the Cushing reflex [51]. Nevertheless, the Cushing reflex is commonly believed to be a protective response to a raised ICP which attempts to maintain cerebral perfusion. The reflex is characterized by arterial hypertension, bradycardia (depression in pulse rate), and increased TPR [52–54].

The reflex begins when cerebral arterioles become compressed due to an increased ICP, diminishing the blood supply to the brain [55]. Insufficient oxygen delivery to the brain activates chemosensitive afferent and hence the sympathetic branch of the autonomic system, causing vasoconstriction through the activation of alpha-1 adrenergic receptors [56]. The constriction raises TPR, resulting in the arterial hypertension. The cerebral and coronary vascular beds are not under sympathetic control; therefore, the increased TPR reduces blood flow to the less vital organs and augments blood flow to the brain and heart [57]. Heart contractility and cardiac output are also increased by the sympathetic stimulation. The ultimate goal of the sympathetic activation is to restore perfusion to the ischemic brain [58].

Meanwhile, the increase in arterial blood pressure is meanwhile detected by baroreceptors in the carotid artery, and parasympathetic response is activated through the stimulation of vagal nerve. This depresses the heart rate and induces bradycardia. Bradycardia may also be contributed by the mechanical stimulation of the vagal nerve due to the increased pressure on the brainstem [57, 59].

3.3 Summary

The current chapter was devoted to cerebral hemodynamics and associated homeostatic mechanisms. Cerebral compliance, cerebral blood flow autoregulation, the baroreceptor reflex, and the Cushing reflex were discussed to some extent. A short part of this chapter was devoted to the pressure-flow relationship within collapsible tubes. The chapter was mainly focused on the theoretical aspects of mechanisms. The practical background associated with the monitoring of the hemodynamics and reflexes and the associated complications will be covered in the next chapter.

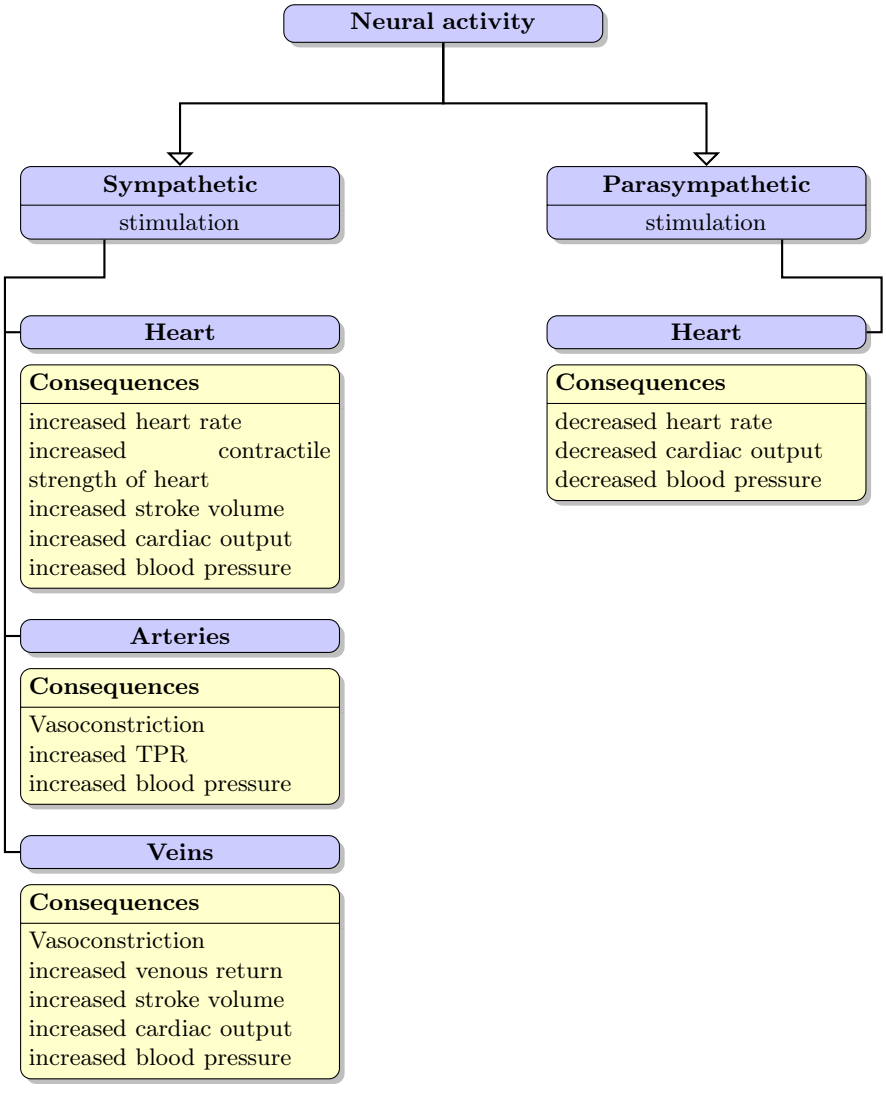

Figure 3.11: The block diagram summarises the effects of the parasympathetic and sympathetic nervous systems on factors that influence mean arterial blood pressure.

CHAPTER 4

Data Analysis and Modelling

If you can dream it, you can do it.

Walt Disney

Preventing secondary brain damages in patients with head trauma necessitates a continuous monitoring of these patients. In the neurointensive care of TBI patients, various biomedical signals are routinely collated, either invasively or non-invasively. Among these signals, ICP, Electrocardiograph (ECG), and arterial blood pressure (ABP) are probably the most important ones mentioned. However, these signals are not direct measurements of cerebral hemodynamics or relevant homeostatic mechanisms. Hence, signal processing and mathematical modelling has become an inevitable part of many investigations in this area.

4.1 Intracranial Pressure Signal Analysis

Intracranial pressure refers to the pressure inside the skull and thus in the brain tissues and CSF. The primary goals of ICP monitoring are identification of intracranial pressure trends and evaluations of therapeutic interventions in order to minimise ischemic injury in a brain-injured patient. ICP is usually maintained in a tight normal range through the shunting of CSF to the subarachnoid space or vasoconstriction of cerebral arterioles. ICP can, therefore, be viewed as a reflection of the capability of craniospinal space to accommodate added volume. It is measured in millimetres of Mercury (mmHg), and for an adult in supine position[10] is normally in the range of $7 - 15$ mmHg. ICP may be measured using different techniques in different sites of the brain (see Figure 4.1). The techniques are listed in Table 4.1.

[10]The supine position is a position of the body; lying down with the face up.

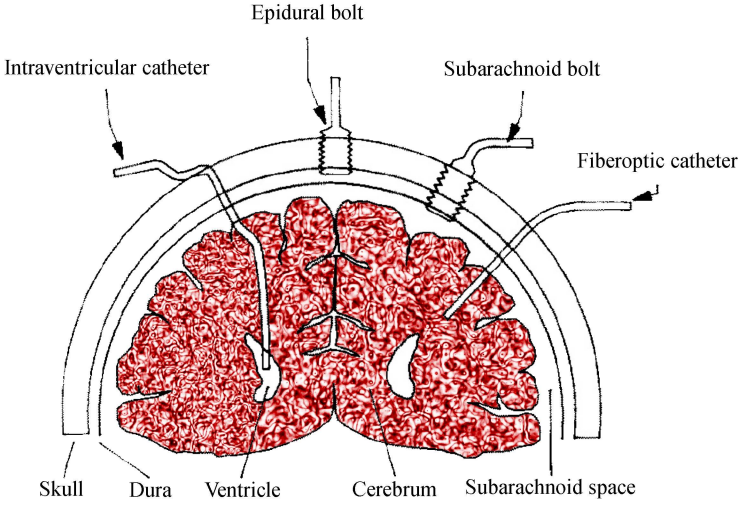

Figure 4.1: Brain sites and ICP measurement. Adapted from [60] with permission.

Table 4.1: Technologies and brain sites in ICP monitoring

Technology
1. External strain gauge
2. Catheter tip (internal strain gauge)
3. Fibre-optic
Location
1. Ventricular
2. Intraparenchymal
3. Subarachnoid
4. Subdural/Extradural

4.1.1 ICP pulse waveform

The ICP signal includes a mean pressure component and some pressure pulsation associated with the cardiac and respiratory cycles (see Figure 4.2). The ICP signal can be regarded as a composed wave which contains the following components:

- *Pulse waveform:* The Pulse waveform includes several harmonics with a fundamental frequency equal to the heart rate. It has been claimed that the amplitude of the fundamental component is useful to evaluate some indices describing cerebrospinal dynamics [38, 61].
- *Respiratory waveform:* The respiratory waveform is related to the frequency of the respiratory cycle ($8 - 20$ cycles per minute).
- *Interaction among cardiac and respiratory components:* Although the existence of a cardiorespiratory interaction in blood pressure has been known for a long

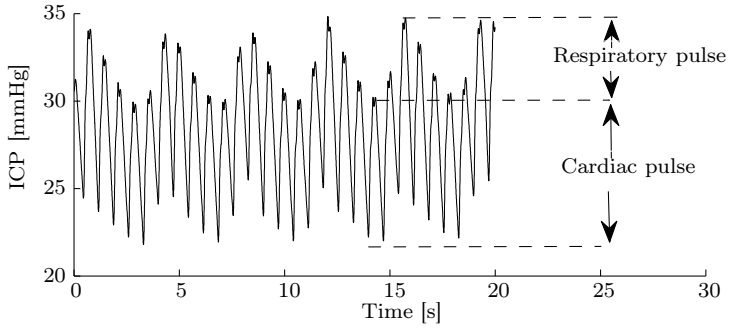

Figure 4.2: ICP signals with emphasize on respiratory and cardiac pulses.

time, and the effect of respiration on the heart rate has been studied by a number of groups [62–64], it has not been paid much attention in case of intracranial pressure.

- *Slow waves:* Slow waves are not precisely defined. All components that have a spectral representation within the frequency limits of 0.05 to 0.0055 Hz (lasting from 20 seconds to 3 minutes) can be classified as slow waves [61].

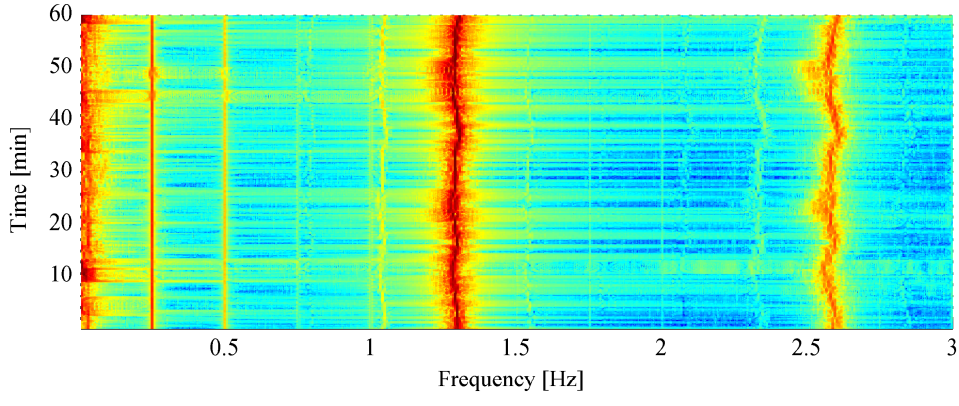

Figure 4.3: Short time Fourier transform of one hour ICP signal collected from a TBI patient. The ICP spectrum contains slow waves with frequency lower than 0.1 Hz, respiratory component (f_R) around 0.25 Hz, cardiac component (f_C) around 1.3 Hz, their higher harmonics and also the interactions between two latter components which are located at $f_C - f_R$, $f_C - 2f_R$, $f_C + f_R$ and so on.

Figure 4.3 presents the short time Fourier transform (STFT) of one hour ICP signal collected from a TBI patient. Note that the ICP spectrum not only contains slow waves with frequency lower than 0.1 Hz, respiratory component (f_R) around 0.25 Hz, cardiac component (f_C) around 1.3 Hz, and also their higher harmonics, but also includes the interactions between two latter components which are located at $f_C - f_R$,

$f_C - 2f_R$, $f_C + f_R$ and so on[11]. The wide red band at the cardiac frequency is a result of the heart rate variability over one time window which makes ICP a quasi-periodic signal.

At present, the mean value of the ICP signal, evaluated on different time scales, is usually used by expertise in NICU to characterize the state of the brain pressure-volume relationship. In fact, only using the mean value of ICP is a process with a high rate of compression which may result in loss of some valuable information. This simply means more information may be available hidden in the intracranial pressure signal, which could improve our understanding about brain homeostatis. Different studies have been carried out, and others are still ongoing, which aim to find ICP features with a greater correlation to the state of the brain. These studies can be categorised into two general classes: firstly, the study of cerebral compliance and secondly, the study of cerebral vasculature and its related homeostatic mechanisms.

4.2 Study of Cerebral Compliance

To get an estimation of cerebral compliance can be assumed to be the ultimate goal in the study of patients with TBI. A known state of cerebral compliance probably reduces the risk of decision making and treatment under uncertainty and can therefore provide better outcomes. Based on this hope a part of the studies into TBI injuries is dedicated to the extraction of features from ICP which are highly correlated with cerebral compliance. The Index of Compensatory Reserve is probably the most appreciated feature among all others.

4.2.1 Index of Compensatory Reserve

RAP (coRrelation coefficient between the Amplitude of the fundamental component and mean Pressure) is a secondary index defined thus:

$$\overline{\mathbf{x}} = (\overline{x}_1\ \overline{x}_2\ \ldots\ \overline{x}_{40})^T$$
$$\overline{\mathbf{y}} = (\overline{y}_1\ \overline{y}_2\ \ldots\ \overline{y}_{40})^T$$

$$RAP = \frac{(\overline{\mathbf{x}} - \mu_{\overline{\mathbf{x}}})^T(\overline{\mathbf{y}} - \mu_{\overline{\mathbf{y}}})}{\sqrt{(\overline{\mathbf{x}} - \mu_{\overline{\mathbf{x}}})^T(\overline{\mathbf{x}} - \mu_{\overline{\mathbf{x}}})}\sqrt{(\overline{\mathbf{y}} - \mu_{\overline{\mathbf{y}}})^T(\overline{\mathbf{y}} - \mu_{\overline{\mathbf{y}}})}}, \tag{4.1}$$

where $\overline{x}_k;\ \ k = 1, \ldots, 40$ refers to the mean of ICP (ICP_{mean}) calculated over a 6-10 seconds averaging period. Similarly, $\overline{y}_k$ denotes the amplitude of the fundamental cardiac component of the ICP waveform (AMP), estimated over the corresponding 6-10 seconds time window. A RAP coefficient calculates the level of linear correlation among 40 consecutive values of AMP and ICP_{mean}.

The RAP coefficient has been proposed by Czosnyka *et al.* [65] as an index to monitor specific states of mechanisms controlling cerebral blood flow circulation and

[11] The rhythmic variation in the heart rate occurring at the frequency of respiration is known as respiratory sinus arrhythmia.

cerebrospinal pressure-volume compensation. AMP is usually estimated by applying the Fast Fourier Transform (FFT) technique to the time series of ICP. However, time domain analysis is another alternative, in which AMP is measured as the peak-to-peak amplitude of the ICP pulsation during one heartbeat. Although both methods are believed to be equivalent in evaluation of AMP [61], some recent studies show that peak-to-peak amplitude of ICP involves the contribution of higher cardiac components as well as the fundamental component [66, 67].

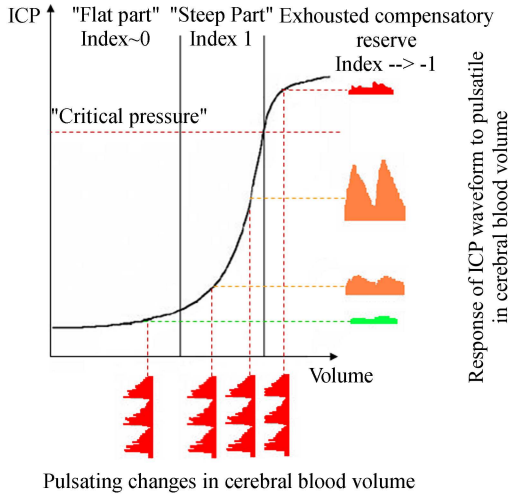

Figure 4.4: The RAP index classifies the volume-pressure curve into three distinct regions corresponding to good pressure-volume compensatory reserve, poor pressure-volume compensatory reserve, and deranged cerebrovascular reactivity. Reproduced from [68] with permission.

The concept behind the RAP index is that each heart beat results in a pulsatile increase in cerebral blood volume and consequently a pulsatile increase in ICP. Therefore, the ICP pulse may be regarded as the intracranial pressure response to this volume increase, and should be representative of the cerebral compliance. Provided that the pulsatile volume increase remains constant over the time, the ICP wave pulse amplitude will increase when cerebral compliance decreases. Since an increased ICP level is also a result of decreased cerebral compliance, a high correlation between the ICP wave pulse amplitude and the ICP level is expected in case of a low cerebral compliance.

The RAP index is not able to define the steepness of the volume-pressure curve as the pressure-volume index (PVI) does. However, it is able to classify the volume-pressure curve into three distinct regions corresponding to *good pressure-volume compensatory reserve, poor pressure-volume compensatory reserve, and deranged cerebrovascular reactivity* (see Figure 4.4). A RAP coefficient close to 0 indicates an asynchrony between variations in AMP and ICP_{mean}, hence implying a good com-

pensatory reserve where fluctuations in intracranial volume cause no or very little changes in ICP. A RAP index around 1 indicates that the changes in AMP and ICP_{mean} are synchronised and therefore indicates a poor compensatory reserve. In this situation, cerebral working point shifts to the right and any further increase in the volume may result in a dramatic increase in ICP. If ICP continuously increases, soon the capacity of cerebral arterioles to dilate in response to the CPP decrements will be exhausted, and arterioles will tend to collapse. This will end up in a decreased AMP and negative RAP values [38, 61, 69]. Figure 4.5 depicts plateau waves in ICP (during maximum vasodilation), where RAP decreases from 1 to 0 as a result of cerebrovascular deterioration.

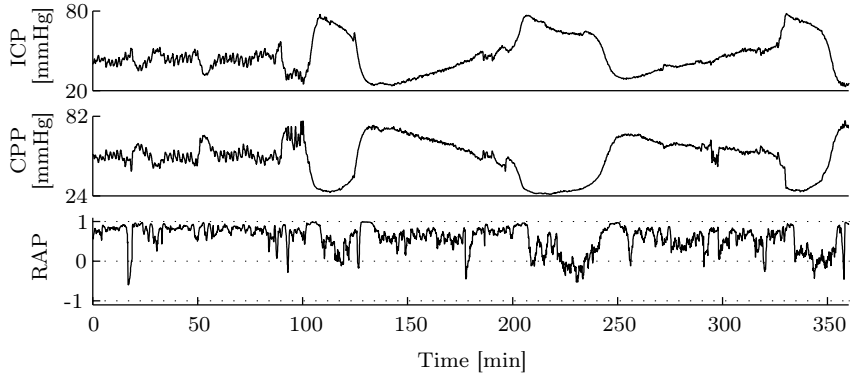

Figure 4.5: During plateau waves of ICP, the RAP decreases from values close to +1 to 0, indicating a state of maximal vasodilation.

Although the index of compensatory reserve seems a breakthrough in determining the cerebral state of compliance, its usability is limited in clinical practices. This limitation comes from the assumption that the pulsatile blood volume remains constant. This is not a valid assumption in severely injured patients with fluctuating cardiovascular function. In clinical studies, however, many investigations have focused on the ICP pulse as a promising parameter to estimate the intracranial pressure-volume state [32].

4.3 Study of Cerebral Vasculature and Circulatory System

The fluctuations in ICP are believed to contain important information on the function of cerebral vasculature and, hence, cerebral blood flow autoregulation. In addition, cerebral compliance is determined by the interaction of the compliances of vascular and CSF compartments. Therefore, the modelling of the cerebral vasculature and the circulatory system are among the main topics of interest in TBI-related investigations.

4.3.1 Index of Cerebrovascular Pressure Reactivity

Another ICP-derived index is called PRx (Pressure Reactivity indeX), which is an indicator of cerebrovascular pressure reactivity. Cerebrovascular pressure reactivity reflects the reaction of smooth muscle tone in the walls of cerebral arteries (dilatation and constriction) to changes in cerebral perfusion pressure. Cerebrovascular pressure reactivity may therefore be used to monitor the cerebral autoregulatory mechanism within the autoregulatory range [41, 70]. With increasing ABP, intact cerebrovascular pressure reactivity results in vasoconstriction and reduction of cerebral blood volume. Under a condition of finite pressure-volume compensatory reserve (e.g. excluding patients with an open external ventricular drain or decompressive craniectomy), this will lead to a decrease in ICP. When cerebrovascular pressure reactivity is impaired, both cerebral blood volume and ICP will follow changes in ABP passively [71].

Although the importance of evaluating cerebrovascular pressure reactivity in patients with TBI has been recognized for many years, its measurement without a manipulation of ABP remains a challenge [70, 72]. In patients receiving mechanical ventilation, however, the presence of slow waves with sufficient magnitudes to provoke vasomotor response has been found to be a great advantage to assess cerebrovascular reactivity without manipulation of ABP [71–76]. For the first time, Czosnyka *et al.* [77] in 1997 introduced a computer-based approach to continuously calculate and monitor cerebrovascular reactivity.

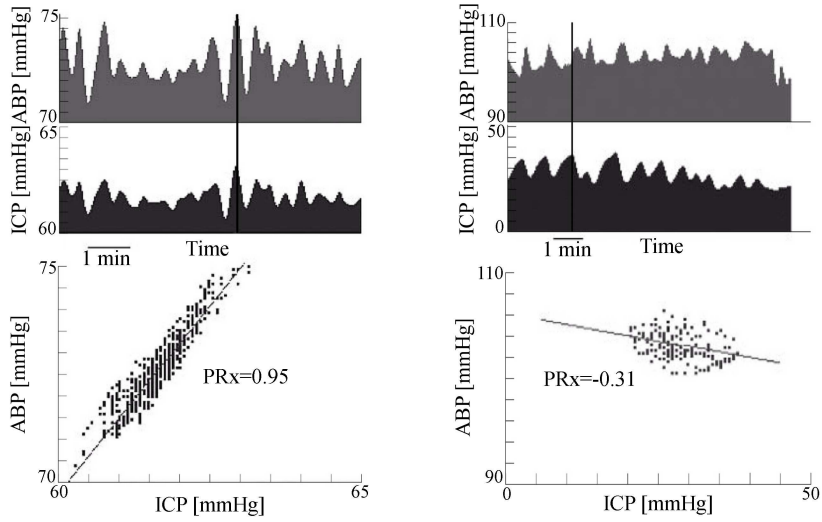

Figure 4.6: PRx calculated as the linear correlation between 40 consecutive 8-second time average data points of ICP and ABP. *Left panel:* A positive PRx (0.95) emphasises impaired cerebrovascular pressure reactivity. *Right panel:* A negative PRx (-0.31) reflects normally reactive vascular bed. Reproduced with permission from [38].

PRx is determined as the linear correlation between 40 consecutive time average data points of ICP and ABP. This is carried out by computational methods similar

to the ones used for RAP index [61]. A positive PRx specifies a positive slope of the regression line between the slow components of ABP and ICP. This has been hypothesised to be the indicator of the disturbed cerebrovascular pressure reactivity, where any change in ABP is passively transmitted to ICP (Figure 4.6, left panel). A negative value of PRx reflects a good pressure reactivity, where changes in ICP and ABP are negatively correlated (Figure 4.6, right panel) [38].

4.3.2 Transfer Function Between ABP and ICP

Applying system identification methods to ICP analysis goes back to 1980 when Portnoy and Chopp described the cerebrovascular system as a black box model [78]. In their model ABP was defined as the chief input to the system, and ICP was considered to be the output response to that stimulus (see Figure 4.7). The idea behind this type of investigation was that the intracranial compliance can have a frequency dependent nature. This means that there may be a particular mechanism running within the cerebrovascular system, i.e. filtering or convolution, which treats different frequencies differently [79].

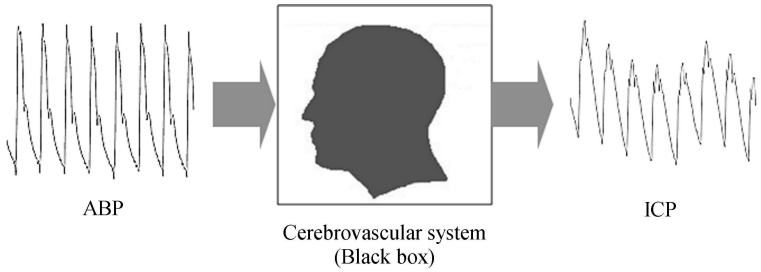

Figure 4.7: Cerebrovascular system has been modeled as a black box with ABP as the input and ICP as the output.

In the conventional nonparametric modelling of the transfer function between ABP and ICP, a FFT-based method, both ABP and ICP are transferred to the frequency domain. ICP and ABP are expressed here as series of sinusoidal waves, including the fundamental cardiac component and its multiple harmonics. The transfer function then can be calculated as the ratio of the cross-spectrum of the input and output ($P_{XY}(\omega)$) to the auto-spectrum of the input ($P_{XX}(\omega)$) in stochastic cases or ratio between the Fourier transforms of the output and input ($Y(\omega)$ and $U(\omega)$) in deterministic cases. An estimate of the transfer function can be obtained from:

$$H(\omega) = \frac{P_{XY}(\omega)}{P_{XX}(\omega)} = \frac{U^*(\omega)Y(\omega)}{U^*(\omega)U(\omega)} = \frac{Y(\omega)}{U(\omega)}, \tag{4.2}$$

where $U^*(\omega)$ is the complex conjugate of $U(\omega)$. The amplitude of the transfer function determines how much pressure is transmitted through the cerebrovascular bed at a given frequency, while its phase indicates the phase shift for that specific frequency component [32, 79].

In 1981, Portnoy and Chopp conducted experiments of raised ICP in cats. They reported an increase in ICP waveform pulse and a simultaneous increase in the amplitude of the transfer function at the fundamental cardiac frequency during the arterial hypercapnia[12] and hypoxia[13] [80]. Further investigation by Portnoy and his colleagues in 1982 showed that in case of low ICP (ICP $<$ 7mmHg) in dogs, there is an amplitude attenuation at the fundamental frequency, while during hypercapnia or intraventricular infusion the transfer function seems more flat in amplitude. They associated this attenuation to functional autoregulatory tone of the precapillary cerebral resistance vessels and interpreted it as a characteristic of the cerebral autoregulation [81].

Employing similar methods, existence of a positive correlation among the raised ICP and the amplitude of the first four cardiac harmonics in both the ICP waveform and transfer function was shown by Takizawa and co-workers [82]. Their study also indicated that ICP become more like a single sine wave when ICP level increases toward 50 mmHg. About the same time as Takizawa, Kasuga by studying cerebrovascular transmission in dogs showed that the lower frequencies of the pulse wave are suppressed during transmission through the intracranial cavity [83].

Later in 1990, Piper adopted the system analysis method of Portnoy and Chopp to a clinical study of cerebrovascular pressure transmission [76]. Studying 1500 ICP records, collected from 30 TBI patients, he recognized four different patterns in the transfer function between ABP and ICP.

- *Low amplitude at both low and high frequencies*
- *Low amplitude at low frequencies and high amplitude at high frequencies*
- *High amplitude at low frequencies and low amplitude at high frequencies*
- *High amplitude at both low and high frequencies*

According to his achievements, both groups with elevated amplitude at the fundamental cardiac frequency were associated with raised ICP, while the other two were associated with ICP less than 15 mmHg. His further investigation in cats demonstrated that three different mechanisms of *active arteriolar vasodilation*, *loss of autoregulatory vascular tone*, and *reduced cerebrovascular transmural pressure* [84] are involved in increasing amplitude of the transfer function at the fundamental cardiac frequency. These mechanisms were found distinguishable by taking the phase shift between the fundamental cardiac frequency components in ABP and ICP into the account. In this experimental model, a negative phase shift was associated with active vasodilation, while decreased transmural pressure did not show an overall phase shift. Finally impaired autoregulation was accompanied by a positive phase shift.

Although various groups have put their efforts behind the study of cerebrovascular pulse transmission, there have been many debates about these techniques. Transfer function by default assumes that there exists a linear transmission from the input to the output. Such an assumption may not be valid when it comes to biosignal considerations, particularly in pathological circumstances [61]. Another drawback of such

[12]Hypercapnia is a condition where there is too much carbon dioxide (CO2) in the blood

[13]Hypoxia is a condition in which the body as a whole (generalized hypoxia) or region of the body (tissue hypoxia) is deprived of adequate oxygen supply

conventional methods is that they are time-invariant and, therefore, not capable of tracking signal evolutions over the time. This disadvantage may be overcome with use of time-varying transfer function models which employ short segments of data in which signals can be assumed to be stationary processes. Time-varying transfer function models are claimed to be capable of identifying inherent nonstationary dynamics in biomedical systems [79].

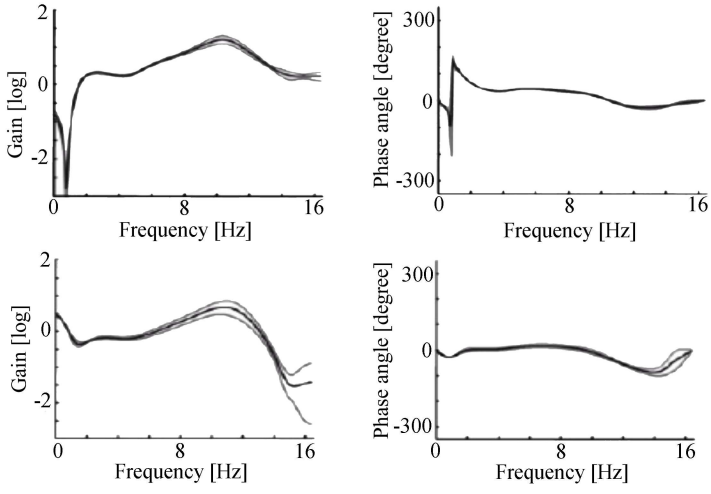

Figure 4.8: Graphs show the transfer function calculated from the ARMA model using 20-second duration of ABP input and ICP output. The average transfer function (calculated over a number of sliding windows) and the standard deviations are indicated by the solid black and the gray lines, respectively. *Top panel:* data recorded during normal ICP. *Bottom panel:* an elevated ICP period. A notch in the gain of the transfer function is visible in top panel when ICP is in the normal range. However, it disappears in the bottom panel for which the ICP level has been increased by bolus injection. Reproduced with permission from [79].

Recently a time-varying transfer function, which devices autoregressive moving average (ARMA) modelling, was applied by Zou and his colleagues to ICP and ABP signals collected from dogs [79]. Their investigations revealed the existence of a deep notch in the amplitude of the transfer function, centred at or near the cardiac frequency for normal ICP. This notch was suppressed when ICP was increased by bolus injection (see Figure 4.8). This is very similar to the results reported by Portnoy in 1982 and Kasuga in 1987. They came to the conclusion that a pulsation absorber may exist in intracranial system in animals for which the target frequency appears to be close to the cardiac frequency. The free movement of cerebrospinal fluid considered as one possible source for such an absorbing mechanism.

4.3.3 Pressure Pulse Wave Propagation Velocity

Pressure pulse wave velocity (PWV), which can simply be calculated by the measurement of pulse wave transit time and the distance travelled by the wave between

two recording sites [85, 86], offers a simple and useful approach to study arterial stiffness. Although the measurement of PWV has got great attention in cardiovascular investigations, until recently it has not been considered in TBI research [87].

When the heart contracts, pressure waves are generated. These pressure waves propagate through the arterial tree with a certain speed, which is independent of the velocity of the blood. A compliant vessel can be modelled as an elastic tube. The pressure pulse velocity within such a vessel can then be obtained by

$$PWV = \sqrt{(1-\sigma^2)\frac{Eh}{2\rho R}}. \tag{4.3}$$

This is a corrected version of the Moens-Korteweg equation, first presented by Bergel [88]. In (4.3), PWV stands for pulse wave velocity, ρ is blood density, h and R introduce wall thickness and mean radius of the vessel, in order. The parameter σ is known as Poisson's ratio, which is the ratio of transverse to longitudinal strain. The Young's modulus of elasticity is represented by E and can be defined as

$$E = \frac{\Delta P}{\Delta R}\frac{2(1-\sigma^2)R_i^2 R_o}{(R_o^2 - R_i^2)}, \tag{4.4}$$

where ΔR is the change in mean radius of the vessel following a pressure change ΔP, R_i is the internal radius, and R_o introduces the external radius [89]. Equation (4.4) can be rewritten as

$$\begin{aligned} E &= \frac{\Delta P}{\Delta R}\frac{2(1-\sigma^2)(R-h/2)^2(R+h/2)}{(R+h/2)^2-(R-h/2)^2} \\ &= \frac{\Delta P}{\Delta R}\frac{(1-\sigma^2)(R^3 - R^2h/2 - Rh^2/4 + h^3/8)}{Rh}. \end{aligned} \tag{4.5}$$

Since the wall thickness of a vessel is small compared to its radius, (4.5) can be approximately simplified to the form

$$E = (1-\sigma^2)\frac{R}{h}E_p, \tag{4.6}$$

where $E_P = R\Delta P/\Delta R$ has been introduced by Peterson *et al.* [90] as the "pressure-strain elastic modulus." By substituting (4.6) into (4.3), the pulse wave velocity can be found in the term of E_p as

$$PWV = (1-\sigma^2)\sqrt{\frac{E_p}{2\rho}}. \tag{4.7}$$

This relationship was previously highlighted by Patel *et al.* [91], but it was also observed during the study of *atherosclerosis risk in communities*, which was conducted in the last decade of the 20th century [92, 93]. The reciprocal of E_p is arterial circumferential extensibility (C_E), also called arterial distensibility, which is formulated as

$$C_E = \frac{\frac{\Delta R}{R}}{\Delta P}. \tag{4.8}$$

The distance x, travelled by the pulse wave, the pulse wave velocity, and the transit time τ are related by $PWV = x/\tau$. Moreover, Lawton has shown that blood vessels extend isovolumetrically indicating that the Poisson's ratio must be about 0.5 [94]. Therefore, assuming a constant blood density, the relationship between the wave transit time on one side and vascular distensibility on the other side can be described by

$$\tau \propto \sqrt{C_E}. \tag{4.9}$$

From (4.9) we learn that pressure waves travel with a lower velocity if arterial distensibility increases and vice versa. Variations in time it takes for a pulse wave to travel from the heart to the cranial space are expected to reflect:

- Changes in the path of larger vessels connecting the heart to the cerebral cavity, τ_1. This path starts from aorta and includes middle cerebral artery (MCA).
- Variations in smaller and more compliant distal cerebral vasculature, τ_2.

thus

$$\tau = \tau_1 + \tau_2. \tag{4.10}$$

Estimation of Cerebrovascular Distensibility

As mentioned before, arterial distensibility is proportional to the square of pulse wave transit time. Hence, variations in arterial distensibility can be tracked by estimating the pulse wave transit time. The time delay between the cerebral blood pressure wave and the ICP wave is assumed to be constant with no effect on the monitored changes of the pulse wave transit time. Therefore, in the absence of measurements from cerebral vessels, the ICP signal can be treated as the wave collected from the interesting site, i.e., distant cerebral arteries and arterioles. The estimation method starts by identifying the characteristic points of the ICP wave. In cardiovascular studies, the foot of the pressure wave is usually selected as the characteristic point. The foot of a wave is identified as the beginning of the initial upstroke. Absence of wave reflections at this point can provide a more accurate estimation of the forward pulse wave velocity [47]. The same approach can be used in the case of the ICP wave.

As a first step, the normalised ECG signal is automatically investigated by a thresholding scheme to locate R-peaks [95]. Within each RR-interval, the ICP signal is filtered through a zero-phase band-pass filter and then analysed to define the maximum pressure point. The foot point is defined to be somewhere between the first R-peak and the maximum point within the interval. A quadratic function is then fitted to the minimum point within the interval and adjacent points, and the analytical minimum point is decided to be the foot point. The time delay between the first R-peak and the foot point is defined as the wave traveling time to the cranial cavity, see Fig. 4.9.

4.3.4 Mathematical Modelling

The existence of complex non-linear relationships among physiological quantities makes qualitative approaches insufficient to extract and reveal important features of

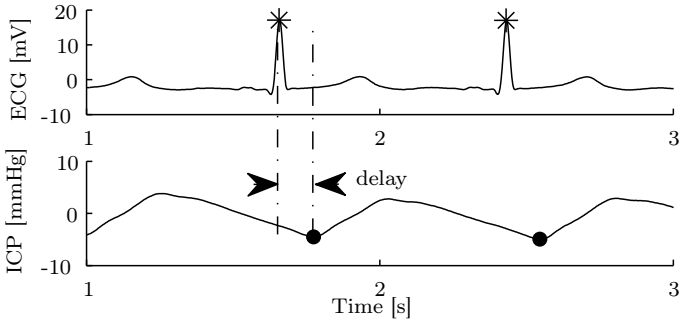

Figure 4.9: The wave transit time to the cranial cavity is measured by the time delay between the first R peak and the ICP foot point within one RR-interval.

cerebral dynamics [10]. Mathematical tools have often showed their intrinsic potential to facilitate the human comprehension of physical systems with high complexity. They definitely have a real potential for modelling physiological systems as well. During the past decades, there have been some works with focus on mathematical modelling of the interaction between intracranial pressure and cerebral hemodynamics [10, 29, 30, 96–100]. Indeed Marmarou and his colleagues ought to be acknowledged for their pioneering work in this area [30, 101].

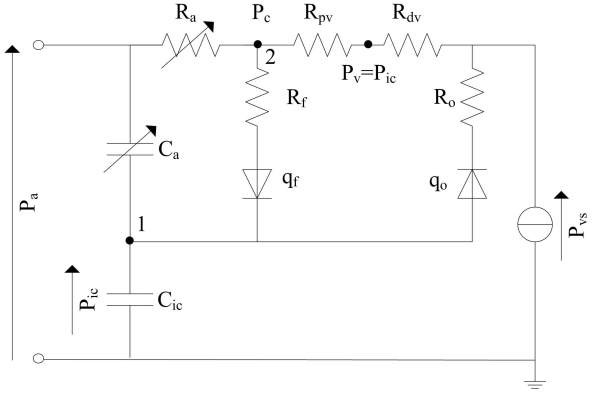

Figure 4.10: Electric analogy of a model of intracranial dynamics proposed by Ursino [10]. Blood flow (q) enters skull in systemic arterial pressure (P_a). Cerebrovascular autoregulation has been modelled through (C_a). (P_{ic}) and (C_{ic}) denote intracranial pressure and compliance, respectively. The formation resistance (R_f) and the outflow resistance (R_o) has been used to model CSF production and reabsorption.

Although several methods have been presented by different research groups, they do not cover the same aspects of intracranial dynamics. Some of them are especially designed to model the cerebrospinal fluid circulation (production and reabsorption) [102, 103]. Some focused on non-linear cerebral compliance [104, 105] and venous collapse [106]; while others tried to take all known phenomena into account [10, 97,

107–109]. A lumped parameter compartmental approach is a common method which has been used by the latter groups to model cerebral dynamics. In this method, pressure interactions among various cerebral compartments are modelled by a set of differential equations. Intracranial volumes and flows are then related to those compartmental pressure differences through compliance and resistance parameters.

The electrical model of Figure 4.10, proposed by Ursino *et al.* in 1997 [10], represents a simple model of intracranial dynamics. The model includes cerebrovascular autoregulation and cerebrospinal fluid circulation as well as cerebral compliance. Cerebral autoregulation is modelled through a regulated capacity (C_a), which stores a certain amount of blood volume in the arterial-arteriolar bed. The regulated resistance (R_a) accounts for pressure drop to capillary pressure (P_c). P_a and q denote systemic arterial blood pressure and cerebral blood flow respectively. CSF formation resistance (R_f) has been used to model CSF production, while CSF reabsorption at venous sinus pressure (P_{vs}) is represented through CSF outflow resistance (R_o). Finally, intracranial pressure (P_{ic}) is determined by the amount of volume stored in the non-linear intracranial compliance (C_{ic}). This volume is resulting from a balance between CSF inflow (q_f), CSF outflow (q_o), and blood volume changes in arterial capacity. Utilizing the above model, self-sustained oscillations of ICP could be produced without any external perturbation. The oscillations simply occurred due to an intrinsic instability of intracranial dynamics resulted from a decrease in intracranial compliance and an increase in CSF outflow resistance while cerebral blood autoregulation was preserved. Ursino used these observations and concluded that the start of a plateau wave is not always evoked by a decrease in systemic blood pressure.

There is no doubt that the above mentioned studies have significant importance in allowing us to improve our physiological knowledge. However, there is still a long way to go in order to obtain a versatile model with a sufficient accuracy and simplicity. Such a model should be capable of describing the different aspects of intracranial dynamics with a sufficient accuracy and still remain simple enough to be routinely employed in medical practices.

4.3.5 Study of The Baroreceptor Reflex Mechanism

The baroreceptor reflex mechanism turns out to be an interesting issue for two reasons when it comes to studies into head trauma. Firstly, the baroreceptor reflex affects the circulatory system and consequently the local autoregulation of blood flow. Secondly, it is controlled by the central nervous system located in the medulla oblongata, the lower half of the brain stem. In fact, the baroreceptor reflex and the cerebral equilibrium mutually affect each other.

Time-Domain BRS Index

Time-domain analysis of BRS is performed over time series of systolic blood pressure (SBP) and RR-intervals of ECG denoted by $\mathbf{x}_{SBP}(n)$ and $\mathbf{x}_{RR}(n)$, accordingly, where $n = 1, 2, ..., N_{max}$. The estimation process is performed in two steps:

- The identification of baroreflex segments (segments which contain changes in SBP and reflexive variations of RR-intervals)

- The BRS estimation from the slope between RR-intervals and SBP

The former task can be conducted either through the sequence technique or the event technique, while the latter may be accomplished by using a local or global approach for slope estimation [110].

The event technique: The event technique is a criterion recently defined for the segmentation of SBP and RR-intervals. This technique consists of identifying segments which exhibit high positive correlation between two series. Each segment needs to meet the required length of beats (N_{min}) and correlation coefficient (r_{min}) to be identified as an event segment. There is no limit on minimum changes in SBP within one RR-interval, though. This means SBP or RR-intervals may not be consecutively increasing or decreasing on a beat-to-beat basis as they are in the sequence technique [111]. The k^{th} identified event segment, $(\mathbf{x}^k_{SBP}, \mathbf{x}^k_{RR})$, is represented by $BE_k,\ k = 1, 2, ..., K$ and is characterised by N_k pairs of values beginning at the index n_k, that is,

$$\begin{aligned} \mathbf{x}^k_{RR} &= [x_{RR}(n_k)\ x_{RR}(n_k+1)\ ...\ x_{RR}(n_k+N_k-1)] \\ \mathbf{x}^k_{SBP} &= [x_{SBP}(n_k-D_k)\ x_{SBP}(n_k-D_k+1)\ ... \\ &\quad x_{RR}(n_k+N_k-D_k-1)]. \end{aligned} \tag{4.11}$$

The parameters of N_k and D_k are selected to meet the boundary conditions while maximizing the slope between $\mathbf{x}^k_{RR}$ and $\mathbf{x}^k_{SBP}$, $\beta(\mathbf{x}^k_{RR}, \mathbf{x}^k_{SBP})$. This can be written as

$$\begin{aligned} (N_k, D_k) &= \underset{N,D}{\operatorname{argmax}}\, \beta(\mathbf{x}^k_{RR}, \mathbf{x}^k_{SBP}) \\ \text{subject to} &\quad N \in [3, 256] \\ &\quad D \in [1, D^k_{max} | T(D^k_{max}) < 5s], \end{aligned} \tag{4.12}$$

where D_k and D^k_{max} refer to the optimum and maximum permitted beat lags for the k^{th} identified event segment, correspondingly. Here $T(D^k_{max})$ stands for the related time lag. The maximum permitted time lag was decided based on several studies which introduced the latency of baroreflex response in human to vary between 1 to 5 seconds [112, 113].

Global approach for slope estimation: The local approach assumes a linear regression between each qualified pair of SBP and RR, i.e.,

$$\mathbf{x}^k_{RR} = a_k \mathbf{x}^k_{SBP} + b_k \mathbf{1}^{N_k} + \mathbf{e}_k, \quad k = 1, 2, ..., K, \tag{4.13}$$

where $\mathbf{1}$ and $\mathbf{e}_k$ are vectors of ones with length N_k and residuals, respectively. The regression parameters are represented by a_k and b_k which are usually estimated through least square methods. The local BRS for the k^{th} segment is estimated as a_k. The final estimate of BRS is obtained by taking the mean of all local BRS's, which is

$$\alpha_L = \frac{1}{K} \sum_{k=1}^{K} a_k. \tag{4.14}$$

Conversely, the global method uses all pairs of data to estimate the slope. Before the BRS estimation, all data are locally treated to remove the mean. The k^{th} zero mean segment $(\hat{\mathbf{x}}^k_{SBP}, \hat{\mathbf{x}}^k_{RR})$ can be represented by

$$\hat{\mathbf{x}}^k_{SBP} = \mathbf{x}^k_{SBP} - \bar{\mathbf{x}}^k_{SBP} \text{ and } \hat{\mathbf{x}}^k_{RR} = \mathbf{x}^k_{RR} - \bar{\mathbf{x}}^k_{RR}, \tag{4.15}$$

where $\bar{\mathbf{x}}^k_{SBP}$ and $\bar{\mathbf{x}}^k_{RR}$) denote the mean value of $\mathbf{x}^k_{SBP}$ and $\mathbf{x}^k_{RR}$, respectively. Later all segments are combined to create two long vectors of $\hat{\mathbf{x}}_{SBP}$ and $\hat{\mathbf{x}}_{RR}$. Removal of the local mean reduces the information dimension of each segment by an order of 1 and emphasises data fluctuations around their local mean. Since the local mean removal pushes all pairs of the data to pass from the origin point, the global measure of BRS can be formulated as

$$\hat{\mathbf{x}}_{RR} = \beta_G \hat{\mathbf{x}}_{SBP} + \mathbf{e}, \tag{4.16}$$

where $\hat{\mathbf{x}}_{SBP} = [\hat{\mathbf{x}}^1_{SBP} \ \ldots \ \hat{\mathbf{x}}^K_{SBP}]$, $\hat{\mathbf{x}}_{RR} = [\hat{\mathbf{x}}^1_{RR} \ \ldots \ \hat{\mathbf{x}}^K_{RR}]$, and $\mathbf{e}$ is a vector of residuals. To estimate β_G, the total least square (TLS) method, in which observational errors on both dependent and independent variables are taken into account, can be utilised. Gouveia *et al.* [110] suggest to eliminate or at least reduce the effect of outliers before applying TLS. According to their approach, the influence of each segment in BRS is evaluated by leaving that segment out of the TLS minimisation. The ratio between the latter result and the TLS estimation, including all segments, is defined as f_k. The k^{th} segment will be classified as an outlier if f_k exceeds the median value more than twice the median absolute deviation (MAD) divided by 0.6745. After removing the outliers, the normalized global BRS can be estimated by

$$\frac{\hat{\mathbf{x}}_{RR,rm}}{\text{MAD}(\hat{\mathbf{x}}_{RR,rm})} = \beta_{G,T,nrm} \frac{\hat{\mathbf{x}}_{SBP,rm}}{\text{MAD}(\hat{\mathbf{x}}_{SBP,rm})} + \mathbf{e}_{rm}, \tag{4.17}$$

where $(\hat{\mathbf{x}}_{SBP,rm}, \hat{\mathbf{x}}_{RR,rm})$ refers to the remaining pairs. The normalization of the variables to their median value of absolute deviation is done in order to scale changes in data and to overcome the sensitivity of TLS [110]. Finally BRS is estimated as

$$\beta_{G,T} = \frac{\text{MAD}(\hat{\mathbf{x}}_{RR,rm})}{\text{MAD}(\hat{\mathbf{x}}_{SBP,rm})} \beta_{G,T,nrm}. \tag{4.18}$$

Frequency-Domain BRS Index

Spontaneous BRS assessment in frequency domain, the so-called α-index, was estimated by calculating the ratio between the powers of the RR and SBP signals in a certain frequency band as follows:

$$\alpha = \sqrt{\frac{\int_{f1}^{f2} S_{RR}(f)df}{\int_{f1}^{f2} S_{SBP}(f)df}}. \tag{4.19}$$

This assessment was accepted to be valid only where the cross-spectral coherence between the two signals was > 0.5 [114]. In (4.19), $S_{RR}(f)$ and $S_{SBP}(f)$ represent

the spectral densities of the RR-interval and SBP fluctuations. A distinction was made between the α index calculated at the low-frequency (LF) range (0.04-0.15 Hz) from the one calculated at the high-frequency (HF) range (0.15-0.4 Hz).

4.4 Summary

Within the current chapter we looked at different possibilities to correlate the monitored signals to the desired processes. While some required just a simple calculation, some others necessitated more extensive modelling of cerebral hemodynamics and cerebral vasculature. Some were found directly correlated to the properties of the brain, i.e. the RAP index, while some others were an indirect measurement of an associated autoregulatory reflex, such as the BRS index. Although each individual extracted feature may associate to a decoupled and simplified subsystem, it is far too simple to accurately reflect the properties of the cerebrospinal system. Hence, an important question still remains unanswered: whether a more accurate monitoring of cerebral hemodynamics is feasible through the combination of different features? The next chapter is devoted to the contributions of this thesis that basically deal with the aforementioned question.

CHAPTER 5

Contributions

> Obstacles are those frightful things you see when you take your eyes off your goal.
>
> Henry Ford

This chapter summarizes the contributions of the thesis. The contributions take the form of four appended papers which basically consider regulatory mechanisms of CBF autoregulation, the baroreceptor reflex, and the Cushing reflex to gather information needed to advance the understanding of various cerebral phenomena. Paper A took advantage of pressure pulse wave propagation velocity, transfer function between ABP and ICP, the RAP index, and the PRx index to study slow waves of intracranial pressure through mechanical properties of cerebral vasculature. The mathematical modelling of cerebral hemodynamics was then combined with the first paper to define the state of cerebral blood flow autoregulatory mechanism in TBI patients with ICP plateau waves. This work was presented in Paper B. Finally, the BRS index was employed in Paper C and D to bind previous studies to investigate the probable effect of the Cushing reflex on the generation and recurrence of ICP plateau waves.

5.1 Publications

A brief summary of the papers, appended to this thesis, is given below.

Paper A *Cerebrovascular Mechanical Properties and Slow Waves of Intracranial Pressure in TBI Patients*

Variations observed in ICP are response of the cerebrospinal system to different stimuli, including myogenic autoregulation of CBF. The myogenic autoregulation is an intrinsic protective reflex to each organ that attempts to maintain a near constant blood flow over the wildly fluctuating ranges of perfusion pressure. This mechanism works through active dilatation and constriction of small arteries and arterioles; hence, the variations in the mechanical properties of these vessels are immediate consequences.

In this article, we argue that the changes in cerebrovascular territory and hence the state of CBF autoregulation can be monitored by estimating the cerebral arterial extensibility and compliance. As a primary contribution of the article, we propose to adopt the concept of PWV to monitor cerebrovascular circumferential extensibility. The second contribution of the work is a model-based framework that incorporates experimental measurements with theoretical aspects to model the interconnection between arterial extensibility and compliance associated to different states of CBF autoregulation.

The results obtained by this study imply that different states of CBF autoregulation and associated regimes within the cerebrovascular system can lead to different types of interrelationship between the slow variations of intracranial pressure, cerebral arterial distensibility, and compliance. Consequently, each of these classes may require different types of treatment on patients with TBI. In addition, the results suggest that during the plateau waves of ICP, the cerebrovascular system may suffer from a partial collapse.

Paper B *A Model-Based Assessment of Cerebral Hemodynamics during Plateau Waves of ICP*

Plateau waves, the acute elevations of ICP, are believed to be initiated by an intact autoregulatory mechanism of cerebral blood flow that migrates the cerebral vasculature toward the maximum vasodilatory phase. The origin of the waves and their prognostic significance, however, are still debated and are of considerable interest to neurologists and neurosurgeons. This consideration besides the results obtained in the Paper A motivates the assessment of cerebral hemodynamics during ICP plateau waves.

This study utilises mathematical models of cerebral hemodynamics and cerebral vasculature. The parameters of the models are tuned based on the collated data from one patient with TBI for whom the recurrence of plateau waves were continuously recorded over eighteen hours. The results emphasise an impaired CBF autoregulation and a partial collapse within the cerebral arterial-arteriolar segment. On account of the fact that flow and pressure drop are negatively correlated within a partially collapsed vessel, this article calls for a more cautious approach to treat TBI patients with ICP plateau waves.

Paper C *Plateau Waves and Baroreflex Sensitivity in Patients with Head Injury: A Case Study*

The interconnection between the blood circulatory system, brain, and autonomic markers from one side and dependency of plateau waves on the circulatory events from the other side raises the question whether baroreflex sensitivity assessment can provide more information about the plateau wave phenomenon.

As the primary contribution of this article, we estimate the sensitivity of baroreceptor reflex during plateau waves and within the intervals between two consecutive waves where intracranial space is exposed to lower levels of ICP. To the best of the authors' knowledge, BRS is never addressed in patients with head trauma for whom plateau waves are recorded and recognized. The sensitivity is investigated over the time domain by employing an event technique and a global approach for slope estimation. The frequency domain estimation of sensitivity is, however, used to differentiate between sympathetic and parasympathetic branches of the autonomic system.

The results, which were verified and validated by the EuroBaVar data set, reveal a very high baroreflex sensitivity during the acute elevations of ICP. It was concluded that this high sensitivity, associated with dominant parasympathetic activity, is caused by a high firing rate of carotid baroreceptors and probably an active Cushing reflex mechanism.

Paper D *Cushing Reflex and Plateau Waves of Intracranial Pressure*

The works cited report a high baroreflex sensitivity during plateau waves of ICP as well as the probable occurrence of a partial collapse in cerebral vascular territory.

The last article reviews the plateau-wave phenomenon by considering the results mentioned above in order to provide a more clear explanation of the phenomenon. Time and frequency domain indices of BRS were used along heart rate variability to discuss the state of the two regulatory mechanisms of baroreceptor reflex and Cushing reflex during plateau waves. Experimental measurements and theoretical concepts of cerebrovascular mechanical properties were then employed to study the effect of the Cushing reflex on the generation of plateau waves.

According to the results obtained in this work, the activation of a Cushing reflex can lead to the generation of so-called plateau waves when CBF autoregulation is exhausted and the cerebral vasculature suffers from a partial collapse. With this conclusion the usefulness of CPP-oriented protocols is once more doubted in case of TBI patients with an impaired CBF autoregulation of cerebral blood flow.

Bibliography

[1] P. L. Reilly and R. Bullock, eds., *Head injury, pathophysiology and management, second edition.* Hodder Arnold, 2005.

[2] D. J. Thurman, C. Alverson, K. A. Dunn, J. Guerrero, and J. E. Sniezek, "Traumatic brain injury in the United States: a public health perspective," *Journal of Head Trauma Rehabilitation*, vol. 14, no. 6, pp. 602–15, 1999.

[3] J. A. Langlois, W. Rutland-Brown, and K. G. Thomas, "Traumatic brain injury in the United States: emergency department visits, hospitalizations, and deaths," tech. rep., Atlanta (GA): Centers for Disease Control and Prevention, National Center for Injury Prevention and Control, 2006.

[4] "TBI incidence," tech. rep., Brain Injury Association of America, www.biausa.org, 2004.

[5] M. J. Rosner, S. D. Rosner, and A. H. Johnson, "Cerebral perfusion pressure: management protocol and clinical results," *J Neurosurg*, vol. 83, pp. 949–62, 1995.

[6] D. W. Marion, *Traumatic Brain Injury.* Thieme, 1999.

[7] P. C. Blumbergs, *Head Injury: pathology and managemen*, ch. Pathology, pp. 41–72. Hodder Arnold, 2nd ed., 2005.

[8] P. R. Cooper, "Delayed brain injury: secondary insults," in *CNS Trauma Status Report* (D. Becker and J. Povlishock, eds.), pp. 217–228, William Byrd Press, 1985.

[9] K. Salci, *Intracranial compliance and secondary brain damage. Experimental and clinical studies in traumatic head injury.* PhD thesis, Uppsala University, 2006.

[10] M. Ursino and C. A. Lodi, "A simple mathematical model of the interaction between intracranial pressure and cerebral hemodynamics," *Journal of Applied Physiology*, vol. 82, no. 4, pp. 1256–69, 1997.

[11] G. Kellie, "An account of the appearances obsereved in the dissection of two of three individuals presumed to have perished in the storm of the third and whose bodies were discovered in the vicinity of Leith on the morning of the 4th, november 1821, with some reflection on the pathology of the brain," *Transactions of Medico-Chirurgical Society of Edinburgh*, pp. 184–69, 1824.

[12] A. Monro, *Observation on the structure and function of nervous system.* Creech & Johnston, Edinburgh, 1783.

[13] G. Burrows, *On disorders of the cerebral circulation and on the connection between affections of the brain and diseases of the heart.* Longman, London, 1846.

[14] B. Schaller and R. Graf, "Different compartments of intracranial pressure and its relationship to cerebral blood flow," *Journal of Trauma: Injury, Infection and Critical Care*, vol. 59, no. 6, pp. 1521–31, 2005.

[15] P. L. Reilly, *Head Injury: pathology and management*, ch. Management of Intracranial Pressure and Cerebral Perfusion Pressure, pp. 93–112. Hodder Arnold, 2nd ed., 2005.

[16] N. Lundberg and H. Troupp, "Continuous recording of the ventricular fluid pressure in patients with severe acute traumatic brain damge. a preliminary report," *J Neurosurg*, vol. 22, no. 6, pp. 581–590, 1965.

[17] N. Lundberg, A. Kjallquist, and C. Bien, "Reduction of increased intracranial pressure by hyperventilation. a therapeutic aid in neurological surgery," *Acta Psychiatr Scand Suppl.*, vol. 34, no. 139, pp. 1–64, 1959.

[18] A. M. Alberico, J. D. Ward, S. C. Choi, A. Marmarou, and H. F. Young, "Outcome after severe head injury. relationship to mass lesions, diffuse injury, and ICP course in pediatric and adult patients," *J Neurosurg*, vol. 67, no. 5, pp. 648–656, 1987.

[19] A. Marmarou, R. L. Anderson, J. D. Ward, S. C. Choi, H. F. Young, H. M. Eisenberg, M. A. Foulkes, L. F. Marshall, and J. A. Jane, "Impact of ICP instability and hypotention on outcome in patients with severe head trauma," *J Neurosurg*, vol. 75, pp. S59–S66, 1991.

[20] L. Marshall, R. W. Smith, and H. M. Shapiro, "The outcome with aggressive treatment in severe head injuries. Part I: the significance of intracranial pressure monitoring," *J Neurosurg*, vol. 50, no. 1, pp. 20–5, 1979.

[21] D. P. Becker, J. D. Miller, and J. D. Ward, "The outcome from severe head injury with early diagnosis and intensive management," *J Neurosurg*, vol. 47, no. 4, pp. 491–502, 1977.

[22] J. D. Miller and J. Garibi, "Intracranial volume/pressure relationships during continous monitoring of ventricular fluid pressure," in *Intracranial Pressure* (B. M. and D. H., eds.), pp. 270–4, Springer-Verlag, Berlin, 1972.

[23] L. H. Pitts, J. V. Kaktis, and R. Juster, "ICP and outcome in patients with severe head injury," in *Intracranial pressure IV* (k. Shulman, A. Marmarou, , and J. Miller, eds.), pp. 5–9, Springer-Verlang, Berlin, 1980.

[24] G. J. Bouma, J. P. Muizelaar, k. Bandoh, and A. Marmarou, "Blood pressure and intracranial pressure-volume dynamics in severe head injury: relationship with cerebral blood flow," *J Neurosurg*, vol. 77, no. 1, pp. 15–9, 1992.

[25] W. J. Gray and M. J. Rosner, "Pressure-volume index as a function of cerebral perfusion pressure. Part 1: The effects of cerebral perfusion pressure changes and anesthesia," *J Neurosurg*, vol. 67, no. 3, pp. 369–76, 1987.

[26] W. J. Gray and M. J. Rosner, "Pressure-volume index as a function of cerebral perfusion pressure. part 2: The effects of low cerebral perfusion pressure and autoregulation," *J Neurosurg*, vol. 67, no. 3, pp. 377–80, 1987.

[27] A. Ikeyama, S. Maeda, A. Ito, K. Banno, H. Nagai, and M. Furuse, "The analysis of the intracranial pressure by the concept of the driving pressure from the vascular system," *Journal of Neurochirurgia*, vol. 21, no. 2, pp. 43–53, 1978.

[28] H. W. Ryder, F. F. Espey, F. V. Kristoff, and J. P. Evans, "Observations on the interrelationships of intracranial pressure and cerebral blood flow," *J Neurosurg*, vol. 8, no. 1, pp. 46–58, 1951.

[29] A. Marmarou, *A theoretical and experimental evaluation of the cerebrospinal fluid system.* PhD thesis, Drexel University, 1973.

[30] A. Marmarou, K. Shulman, and J. LaMorgese, "Computational analysis of compliance and outflow resistance of the cerebrospinal fluid system," *J Neurosurg*, vol. 43, pp. 523–534, 1975.

[31] J. D. Miller and J. Garibi, "Induced changes of cerebrospinal fluid volume: effects during continous monitoring of ventricular fluid pressure," *Archive of Neurology*, vol. 28, pp. 265–9, 1973.

[32] I. R. Piper, *Head Injury: pathology and management*, ch. Intracranial pressure and elastance, pp. 93–112. Hodder Arnold, 2nd ed., 2005.

[33] J. D. Miller, "Volume and pressure in the craniospinal axis," *Clinical Neurosurgery*, vol. 22, pp. 76–105, 1975.

[34] J. D. Miller, P. J. Leech, and J. D. Pickard, "Volume pressure response in various experimental and clinical conditions," in *Intracranial Pressure II* (L. M., P. U., and B. M., eds.), pp. 97–9, Springer-Verlag, Berlin, 1975.

[35] J. D. Miller and J. D. Pickard, "Intracranial volume/pressure studies in patients with head injury," *Injury*, vol. 5, pp. 265–8, 1974.

[36] C. J. J. Avezaat and J. H. M. van Eijndhoven, "The role of the pulsatile pressure variations in intracranial pressure monitoring," *Neurosurgical Review*, vol. 9, no. 1-2, pp. 113–120, 1986.

[37] M. Balestreri, M. Czosnyka, L. A. Steiner, E. Schmidt, P. Smielewski, B. Matta, and J. D. Pickard, "Intracranial hypertension: what additional information can be derived from ICP waveform after head injury?," *Acta Neurochirurgica*, vol. 146, pp. 131–141, 2004.

[38] M. Czosnyka and J. D. Pickard, "Monitoring and interpretation of intracranial pressure," *J. Neurol. Neurosurg. Psychiatry*, vol. 75, pp. 812–821, 2004.

[39] M. Czosnyka, P. Wollk-Laniewski, L. Batorski, and W. Zaworski, "Analysis of intracranial pressure waveform during infusion test," *Acta Neurochirurgica*, vol. 93, no. 3-4, pp. 140–5, 1988.

[40] E. Cheraskin, *Human Health and Homeostasis: Body Balance, Measuring and Mapping the Steady State*. Clayton College/Natural Reader Press, 1st ed., September 1999.

[41] O. B. Paulson, "Cerebral autoregulation," *Cerebrovasc Brain Metab Rev*, vol. 2, no. 2, pp. 161–92, 1990.

[42] R. E. Klabunde, *Cardiovascular Physiology Concepts*. Lippincott Williams & Wilkins, 2005.

[43] M. Reinhard, M. Roth, T. Müller, M. Czosnyka, J. Timmer, and A. Hetzel, "Cerebral autoregulation in carotid artery occlusive disease assessed from spontaneous blood pressure fluctuations by the correlation coefficient index," *Stroke*, vol. 34, no. 9, pp. 2138–44, 2003.

[44] L. A. Steiner, J. P. Coles, A. J. Johnston, D. A. Chatfield, P. Smielewski, T. D. Fryer, F. I. Aigbirhio, J. C. Clark, J. D. Pickard, D. K. Menon, and M. Czosnyka, "Assessment of cerebrovascular autoregulation in head-injured patients: a validation study," *Stroke*, vol. 34, no. 10, pp. 2404–9, 2003.

[45] H. Low and Y. Chew, "Pressure/flow relationships in collapsible tubes: effects of upstream pressure fluctuations," *Medical and Biological Engineering and Computing*, vol. 29, pp. 217–221, 1991.

[46] M. Heil and O. E. Jensen, *Flow Past Highly Compliant Boundaries and in Collapsible Tubes*. Springer, 1st ed., 2003.

[47] W. W. Nichols and M. F. O'Rourke, *McDonald's blood flow in arteries : theoretical, experimental, and clinical principles*. Hodder Arnold, 5th ed. ed., 2005.

[48] A. I. Katz, Y. Chen, and A. H. Moreno, "Flow through a collapsible tube experimental analysis and mathematical model," *Biophys J*, vol. 9, no. 10, pp. 1261–79, 1969.

[49] T. W. Rooke and H. V. Sparks, *Medical Physiology*, ch. 18, pp. 290–308. Lippincott Williams & Wilkins, 2nd ed., March 2003.

[50] H. Cushing, "Concerning a definite regulatory mechanism of the vaso-motor center which controls blood pressure during cerebral compression," *Johns Hopkins Hosp. Bull.*, vol. 126, pp. 290–2, 1901.

[51] R. A. Little and B. Öberg, "Arterial baroreceptor reflex function during elevation of intracranial pressure," *Acta Ohysiol Scand*, vol. 112, pp. 27–32, 1981.

[52] C. F. Su, C. T. Hu, and H. I. Chen, "Effects of intracranial hypertension on steady and pulsatile haemodynamics in dogs," *Clin. Exp. Pharmacol. Physiol.*, vol. 26, no. 11, pp. 898–902, 1999.

[53] H. I. Chen and D. I. Wang, "Systemic and pulmonary hemodynamic responses to intracranial hypertension," *Amer. J. Physiol.*, vol. 247, no. 5, pp. H715–H721, 1984.

[54] T. B. Ducker and R. L. Simmons, "Increased intracranial pressure and pulmonary edema. Part 2. the hemodynamic response of dogs an monkeys to increased intracranial pressure," *J. Neurosurg.*, vol. 28, no. 2, pp. 118–123, 1968.

[55] C. J. Dickinson, "Reappraisal of the Cushing reflex: the most powerful neural blood pressure stabilizing system," *Clin. Sci.*, vol. 79, no. 6, pp. 543–50, 1990.

[56] O. L. Woodman and S. F. Vatner, "Coronary vasoconstriction mediated by alpha 1- and alpha 2-adrenoceptors in conscious dogs," *Amer. J. Physiol.*, vol. 253, no. 2, pp. H388–H393, 1987.

[57] M. Ursino, M. Giannessi, M. Frapparelli, and E. Masosso, "Effect of Cushing response on systemic arterial pressure," *IEEE Eng Med and Biol Mag*, vol. 28, no. 6, pp. 63–71, 2009.

[58] P. Brodal, "The central nervous system: Structure and function," *Oxford University Press US*, pp. 369–96, 2004.

[59] J. G. Hackett, F. M. Abboud, A. L. Mark, P. G. Schmid, and D. D. Heistad, "Coronary vascular responses to stimulation of chemoreceptors and baroreceptors: Evidence for reflex activation of vagal cholinergic innervation," *Circ Res*, vol. 31, no. 1, pp. 8–17, 1972.

[60] D. J. Doyle and P. W. S. Mark, "Analysis of intracranial pressure," *Journal of Clinical Monitoring and Computing*, vol. 8, pp. 81–90, 1991. 10.1007/BF01618093.

[61] M. Czosnyka, P. Smielewski, I. Timofeev, A. Lavinio, E. Guazzo, P. Hutchinson, and J. D. Pickard, "Intracranial pressure: More than a number," *Journal of Neurosurgical Focus*, vol. 22, no. 5, pp. 1–7, 2007.

[62] J. Erlanger and E. G. Festerling, "Respiratory waves of blood pressure, with an investigation of a method for making continuous blood pressure records in man," *J. Exp. Med.*, vol. 15, pp. 370–88, April 1912.

[63] V. N. Smelyanskiy, D. G. Luchinsky, A. Stefanovska, and P. V. E. McClintock, "Inference of a nonlinear stochastic model of the cardiorespiratory interaction," *Physical Review Letters*, vol. 94, March 2005.

[64] U. Zwiener, B. Lüthke, R. Bauer, D. Hoyer, A. Richter, and H. Wagner, "Heart rate fluctuations of lower frequencies than the respiratory rhythm but caused by it," *Pflügers Archiv European Journal of Physiology*, vol. 429, pp. 455–61, February 1995.

[65] M. Czosnyka, J. D. Pickard, and M. Williamson, "Monitoring of cerebrospinal dynamics using continuous analysis of intracranial pressure and cerebral perfusion pressure in head injury," *Acta Neurochirurgica*, vol. 126, no. 2-4, pp. 113–9, 1994.

[66] S. Holm and P. K. Eide, "The frequency domin versus time domain methods for processing of intracranial pressure (ICP) signals," *Medical Engineering & Physics*, vol. 30, no. 2, pp. 164–170, 2007.

[67] S. Shahsavari and T. McKelvey, "Frequency interpretation of tidal peak in intracranial pressure wave," in *Proc. 30th Annu. Int. Conf. IEEE*, pp. 2689–92, Eng. Med. Biol. Soc., 2008.

[68] M. Balestreri, M. Czosnyka, L. A. Steiner, E. Schmidt, P. Smielewski, B. Matta, and J. D. Pickard, "Intracranial hypertension: what additional information can be derived from ICP waveform after head injury?," *Acta Neurochirurgica*, vol. 146, pp. 131–141, 2004.

[69] M. Czosnyka, L. Steiner, M. Balestreri, E. Schmidt, P. Smielewski, P. Hutchinson, and J. D. Pickard, "Concept of true CP in monitoring and prognostication in head trauma," *Intracranial Pressure and Brain Monitoring XII*, vol. 95, pp. 341–344, May 2006.

[70] G. E. Cold and F. T. Jensen, "Cerebral autoregulation in unconscious patients with brain injury," *Acta Anaesthesiol Scand*, vol. 22, no. 3, pp. 270–80, 1978.

[71] C. Zweifel, A. Lavinio, L. Steiner, D. Radolovich, P. Smielewski, I. Timofeev, M. Hiler, M. Balestreri, P. Kirkpatrick, J. Pickard, P. Hutchinson, and M. Czosnyka, "Continuous monitoring of cerebrovascular pressure reactivity in patients with head injury," *Neurosurg Focus*, vol. 25, no. 4, pp. 1–8, 2008.

[72] J. Overgaard and W. A. Tweed, "Cerebral circulation after head injury. 1. cerebral blood flow and its regulation after closed head injury with emphasis on clinical correlations," *J Neurosurg*, vol. 41, no. 5, pp. 531–41, 1974.

[73] R. Aaslid, K. F. Lindegaard, W. Sorteberg, and H. Nornes, "Cerebral autoregulation dynamics in humans," *Stroke*, vol. 20, no. 1, pp. 45–52, 1989.

[74] N. Lundberg, "Continuous recording and control of ventricular fluid pressure in neurosurgical practice," *Acta Psychiatr Neurol Scand Suppl*, vol. 36, no. 149, pp. 1–193, 1960.

[75] J. P. Muizelaar, J. D. Ward, A. Marmarou, P. G. Newlon, and A. Wachi, "Cerebral blood flow and metabolism in severely head-injured children," *J Neurosurg*, vol. 71, no. 1, pp. 72–6, 1989.

[76] I. R. Piper, J. D. Miller, N. M. Dearden, J. R. Leggate, and I. Robertson, "Systems analysis of cerebrovascular pressure transmission: an observational study in head-injured patients," *J Neurosurg*, vol. 73, pp. 871–80, December 1990.

[77] M. Czosnyka, P. Smielewski, P. Kirkpatrick, R. Laing, D. Menon, and J. D. Pickard, "Continuous assessment of the cerebral vasomotor reactivity in head injury," *J Neurosurg*, vol. 41, no. 1, pp. 11–9, 1997.

[78] M. Chopp and H. D. Portnoy, "System analysis of intracranial pressure. comparison with volume-pressure test and CSF-pulse amplitude analysis," *J Neurosurg*, vol. 53, no. 4, pp. 516–527, 1980.

[79] R. Zou, E. H. Park, E. M. Kelly, M. Egnor, M. E. Wagshul, and J. R. Madsen, "Intracranial pressure waves: characterization of a pulsation absorber with notch filter properties using systems analysis," *J Neurosurg: Pediatrics*, vol. 2, no. 1, pp. 83–94, 2008.

[80] H. D. Portnoy and M. Chopp, "Cerebrovascular fluid pulse wavefrom analysis during hypercapnia and hypoxia," *J Neurosurg*, vol. 9, no. 1, pp. 14–27, 1981.

[81] H. D. Portnoy, M. Chopp, C. Branch, and M. B. Shannon, "Cerebrospinal fluid pulse waveform as an indicator of cerebral autoregulation," *J Neurosurg*, vol. 56, no. 5, pp. 668–678, 1982.

[82] H. Takizawa, T. Gabra-Sanders, and J. D. Miller, "Changes in cerebrospinal fluid pulse wave spectrum associated with raised intracranial pressure," *J Neurosurg*, vol. 20, no. 3, pp. 355–61, 1987.

[83] Y. Kasuga, H. Nagai, Y. Hasegwa, and M. Nitta, "Transmission characterestics of pulse waves in intracranial cavity of dogs," *J Neurosurg*, vol. 66, no. 6, pp. 907–14, 1987.

[84] I. R. Piper, K. H. Chan, I. R. Whittle, and J. D. Miller, "An experimental study of cerebrovascular resistance, pressure transmission and craniospinal compliance," *J Neurosurg*, vol. 32, no. 5, pp. 805–16, 1993.

[85] R. Asmar, *Arterial Stiffness and Pulse Wave Velocity. Clinical applications.* Elsevier, 1999.

[86] R. Asmar, A. Benetos, J. Topouchian, P. Laurent, B. Pannier, A. M. Brisac, R. Target, and B. I. Levy, "Assessment of arterial distensibility by automatic pulse wave velocity measurement: Validation and clinical application studies," *Hypertension*, vol. 26, pp. 485–490, 1995.

[87] S. Shahsavari, T. McKelvey, B. Rydenhag, and C. E. Ritzèn, "Cerebrovascular mechanical properties and slow waves of intracranial pressure in TBI patients," *IEEE Transactions on Biomedical Engineering*, vol. 58, no. 7, pp. 2072–2082, 2011.

[88] D. H. Bergel, *The visco-elastic properties of the arterial wall.* PhD thesis, University of London, 1960.

[89] D. H. Bergel, "The static elastic properties of the arterial wall," *J Physiol.*, vol. 156, no. 3, pp. 445–57, 1961.

[90] L. H. Peterson, R. E. Jensen, and J. Parnell, "Mechanical properties of arteries in vivo," *Circ Res*, vol. 8, no. 3, pp. 622–639, 1960.

[91] D. J. Patel, F. M. D. Freitas, J. C. Greenfield, and D. L. Fry, "Relationship of radius to pressure along the aorta in living dogs," *J Appl Physiol*, vol. 18, no. 6, pp. 1111–1117, 1963.

[92] J. K. Liao, M. A. Bettmann, T. Sandor, J. I. Tucker, S. M. Coleman, and M. A. Creager, "Differential impairment of vasodilator responsiveness of peripheral resistance and conduit vessels in humans with atherosclerosis," *Circ Res*, vol. 68, no. 4, pp. 1027–1034, 1991.

[93] D. K. Arnett, L. E. Chambless, H. Kim, G. W. Evans, and W. Riley, "Variability in ultrasonic measurements of arterial stiffness in the atherosclerosis risk in communities study," *Ultrasound in Medicine and Biology*, vol. 25, no. 2, pp. 175 – 180, 1999.

[94] R. W. Lawton, "Thermoelastic behavior of isolated aortic strips of the dog," *Circ Res*, vol. 2, no. 4, pp. 344–53, 1954.

[95] S. Shahsavari and T. McKelvey, "Harmonics tracking of intracranial and arterial blood pressure," in *Proc. 30th Annu. Int. Conf. IEEE*, pp. 2644–7, Eng. Med. Biol. Soc., 2008.

[96] M. L. Daley, R. L. Pasley, and C. W. Leffler, "Modeling cyclic variation of intracranial pressure," in *Proceedings of the 23rd Annual International Conference of the IEEE*, vol. 1, pp. 251–4, Engineering in Medicine and Biology Society, 2001.

[97] M. Ursino and P. D. Giammarco, "A mathematical model of the relationship between cerebral blood volume and intracranial changes-the generation of plateau waves," *Ann Biomed Eng.*, vol. 19, no. 1, pp. 15–42, 1991.

[98] M. Ursino, C. A. Lodi, S. Rossi, and N. Stocchetti, "Intracranial pressure dynamics in patients with acute brain damage," *Journal of Applied Physiology*, vol. 82, no. 4, pp. 1270–82, 1997.

[99] W. Wakeland and B. Goldstein, "A computer model of intracranial pressure dynamics during traumatic brain injury that explicity models fluid flows and volumes," in *Intracranial Pressure and Brain Monitoring XII*, vol. 95, 2006.

[100] W. Wakeland, J. McNames, M. Aboy, D. Hollemon, and B. Goldstein, "Modeling intracranial fluid flows and volumes during traumatic brain injury to better understand pressure dynamics," in *Proceedings of the 25th Annual International Conference of the IEEE*, vol. 3, pp. 402–5, Engineering in Medicine and Biology Society, 2003.

[101] A. Marmarou, K. Shulman, and R. M. Rosende, "A nonlinear analysis of the cerebrospinal fluid system and intracranial pressure dynamics," *J Neurosurg*, vol. 48, pp. 332–344, 1978.

[102] J. D. Charlton, H. A. Guess, J. D. Mann, H. T. Nagle, and R. N. Johnson, "A pressure controller for estimating parameters for a nonlinear CSF model," *IEEE Trans. Biomed.*, vol. 35, no. 9, pp. 752–5, 1988.

[103] J. D. Mann, A. B. Butler, J. E. Rosenthal, C. J. Maffeo, R. N. Johnson, , and N. H. Bass, "Regulation of intracranial pressure in rat, dog and man," *Ann Neurol*, vol. 3, no. 2, pp. 156–65, 1978.

[104] C. J. J. Avezaat and J. H. M. van Eijndhoven, "Cerebrospinal fluid pulse pressure and intracranial volume-pressure relationships," *Journal of Neurology, Neurosurgery & Psychiatry*, vol. 42, no. 8, pp. 687–700, 1979.

[105] W. D. Lakin, J. Yu, and P. L. Penar, "Analysis and validation of a mathematical model for intracranial pressure dynamics," *Mathematical and Computer Modelling of Dynamical Systems*, vol. 5, no. 1, pp. 55–73, 1999.

[106] M. Chopp and H. D. Portnoy, "Starling resistor as a model of the cerebrovascular bed," in *Intracranial Pressure V* (I. Ishii, H. Nagai, and M. Brock, eds.), pp. 174–9, Springer-Verlag, 1983.

[107] M. Czosnyka, N. G. Harris, J. D. Pickard, and S. Piechnik, "CO_2 cerebrovascular reactivity as a function of perfusion pressure - a modelling study," *Acta Neurochirurgica*, vol. 121, no. 3-4, pp. 159–65, 1993.

[108] H. Haffman, "Biomathematics of intracranial CSF and hemodynamics, simulation and analysis with the aid of a mathematical model," *Acta Neurochirurgica*, vol. 40, pp. 117–30, 1987.

[109] S. Sorek, J. Bear, and Z. Karni, "Resistances and compliances of a compartmental model of the cerebrovascular system," *Ann. Biomed. Eng.*, vol. 17, pp. 1–12, 1989.

[110] S. Gouveia, A. P. Rocha, P. Laguna, and P. Lago, "Time domain baroreflex sensitivity assessment by joint analysis of spontaneous SBP and RR series," *Biomedical Signal Processing and Control*, vol. 4, no. 3, pp. 254–61, 2009.

[111] M. D. Rienzo, P. Castiglioni, G. Mancia, A. Pedotti, and G. Parati, "Advancements in estimating baroreflex function exploring different aspects of autonomic control of the heart through the sequence technique," *IEEE Eng. Med. Biol.Mag.*, vol. 20, pp. 25–32, 2001.

[112] B. E. Westerhof, J. Gisolf, W. Stok, K. Wesseling, and J. Karemaker, "Time-domain cross-correlation baroreflex sensitivity: performance on the EUROBAVAR data set," *Journal of Hypertension*, vol. 22, no. 7, pp. 1371–80, 2004.

[113] T. Wu, C. Chen, and T. Kao, "Baroreflex sensitivity evaluation by Volterra Wiener model and the Laguerre expansion technique," *Computers in cardiology*, pp. 741–4, 2008.

[114] Y. C. Tzeng, P. Y. W. Sin, S. J. E. Lucas, and P. N. Ainslie, "Respiratory modulation of cardiovagal baroreflex sensitivity," *J Appl Physiol*, vol. 107, pp. 718–24, 2009.